nature cell biology

A global analysis of cross-talk in a mammalian cellular signalling network

Madhusudan Natarajan[1,2], Keng-Mean Lin[1,2], Robert C. Hsueh[1,2], Paul C. Sternweis[1,2] and Rama Ranganathan[1,3,4]

Cellular information processing requires the coordinated activity of a large network of intracellular signalling pathways. Cross-talk between pathways provides for complex non-linear responses to combinations of stimuli, but little is known about the density of these interactions in any specific cell. Here, we have analysed a large-scale survey of pathway interactions carried out by the Alliance for Cellular Signalling (AfCS) in RAW 264.7 macrophages. Twenty-two receptor-specific ligands were studied, both alone and in all pairwise combinations, for Ca^{2+} mobilization, cAMP synthesis, phosphorylation of many signalling proteins and for cytokine production. A large number of non-additive interactions are evident that are consistent with known mechanisms of cross-talk between pathways, but many novel interactions are also revealed. A global analysis of cross-talk suggests that many external stimuli converge on a relatively small number of interaction mechanisms to provide for context-dependent signalling.

To define 'complexity' in terms of cellular signalling consider all possible combinations of input stimuli that might initiate signalling events in a cell as a set of unique 'messages' that can be sent by the external environment. Even if we simplify the analysis by treating stimuli as binary inputs, the number of such messages grows dramatically with the number of stimuli — for even 20 inputs, over a million possible unique combinations are possible. How does a cell process this enormous number of potential messages in making output responses? At the limit of minimal complexity, signalling events initiated by ligands could be entirely independent of one another, with no cross-talk or mutual influence. In this case, the response to any combination of stimuli requires knowledge of only the single ligand responses as any unsaturated response must be simply a linear, weighted summation of these responses. This mechanistic independence of transduction events does not prevent the cell from having many output states to combinations of stimuli — it only means that all the output states are predictable from combinations of single ligand responses. At the limit of maximal complexity, however, the responses of ligands would be fully context-dependent; that is, the response to any given ligand depends on the specific background of others. In this case, the total cellular response to any combination of stimuli is fundamentally unpredictable from responses to other combinations of ligands. Each ligand combination produces an irreducible unique output state and knowledge of single ligand response is insufficient to describe any of these states.

This operational definition of complexity — the unpredictability of responses to arbitrary combinations of stimuli given knowledge of responses to their simpler combinations — is intimately linked to the wiring complexity of the underlying signalling system. The more unpredictable the response to combinations of stimuli, the more interconnected and structurally complex the transduction network must be. To provide an experimental assessment of functional interactions between stimuli in one cell type, the Alliance for Cellular Signaling (AfCS, http://www.signaling-gateway.org/)[1] carried out systematic measurements of output responses of RAW 264.7 macrophages to the application of 22 receptor-specific ligands and all 231 pairwise combinations of these ligands. The ligands were identified through examination of the literature, receptor expression studies and preliminary dose-response experiments (see Supplementary Information, Fig. S1). Selected agonists provide for stimulation of a diverse set of signalling pathways (Toll-like receptors (TLRs), G protein-coupled receptors (GPCRs), cytokine receptors and tyrosine kinase receptors; see Supplementary Information, Table S1), many of which are co-activated during physiological signalling events (see Supplementary Information, Table S2). Output measurements fell into two categories: (1) final outputs, comprised of measurements of secretion of 18 cytokines; and (2) intermediate outputs, comprised of the kinetics of intracellular calcium mobilization and cAMP synthesis and the phosphorylation of 21 signalling proteins. Analysis of these data describe a basic architecture of the signalling network in which only a few input stimuli are able to independently control cellular outputs and the majority of inputs primarily act as modulators of signalling. The data suggest that the regulatory cross-talk between signalling cascades may be comprised of a limited number of interaction mechanisms and thus provide the basis for a systematic dissection of these mechanisms.

[1]Department of Pharmacology, University of Texas Southwestern Medical Center, Dallas, TX 75390–9050, USA. [2]The Alliance for Cellular Signalling, University of Texas Southwestern Medical Center, Dallas TX 75390, USA. [3]Howard Hughes Medical Institute, University of Texas Southwestern Medical Center, Dallas, TX 75390–9050, USA. [4]Correspondence should be addressed to R.R. (e-mail: rama.ranganathan@utsouthwestern.edu)

Received 23 February 2006; accepted 18 April 2006; published online 14 May 2006; DOI: 10.1038/ncb1418

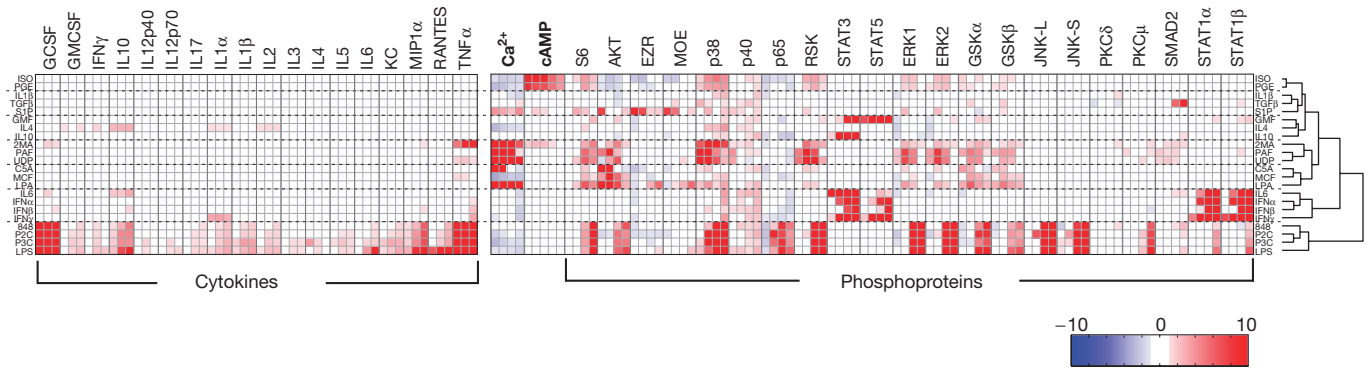

Figure 1 The single ligand screen in RAW 264.7 cells. The matrix shows the experimental responses (columns) of RAW cells to stimulation with the 22 ligands (rows) that comprise the scope of the AfCS study. Responses are in *Z*-scores (see text) that represent the number of standard deviations that each experimental result is removed from unstimulated controls. Each block of columns represents a time series of observation (Ca^{2+} – rising phase and peak, initial falling phase, slow decay to steady state, plateau; cAMP – 0.33, 0.66, 1.5, 5 and 20 min; phosphorylation – 1, 3, 10 and 30 min; cytokine production - 2, 3 and 4 h). The matrix is hierarchically clustered by ligand, with functional groups divided by dashed lines. The colour scale ranges from – 10σ (blue) to + 10σ (red), with all insignificant values within ± 1σ in white.

RESULTS

The single ligand screen

A clustered matrix representation of the single ligand screen — the profiling of output responses to all 22 ligands applied individually — is shown in Fig. 1. Each pixel of the matrix shows the mean signal for one experimentally measured variable (a column) on stimulation with one ligand (a row). The measured variables came from several experimental assays that differed in units of measurement, signal-to-noise ratio and intrinsic day-to-day variability – for example, measurements of intracellular Ca^{2+} (in nM) were typically rapid (seconds), showed good dynamic range and were sampled every 3 s for 10 min. In contrast, measurements of phosphoprotein responses (fold change over basal) over a time-scale of many minutes showed relatively weaker dynamic range, and were sampled only four times over 30 min. Thus, we transformed all raw measurements into *Z*-scores to provide a uniform statistical representation of the data suitable for comparison (see Methods). Hierarchical clustering reveals a robust classification of ligands into known functional groups (separated by dotted lines) on the basis of their output response profiles. Ligands for the TLRs, lipopolysaccharide (LPS), PAM2CSK4 (P2C), PAM3CSK4 (P3C) and resiquimod (848) emerge as a single cluster distinguished by their dominant action in cytokine secretion and similar patterns of protein phosphorylation. TLRs signal through the proximal adaptor protein MyD88, which results in activation of NF-κB and MAP kinase pathways[2]. Consistent with this, *Z*-scores for the TLR ligands show time-evolving phosphorylation of an NF-κB signalling component (p65 subunit), ribosomal S6 protein and S6 kinase (RSK), proteins in the phophatidylinositol-3-OH-kinase (PI(3)K) pathway (Akt, GSKα and GSKβ) and MAP kinase signalling proteins (p38MAPK, ERK1, ERK2, JNKL, JNKS), as well as cytokine production. The interferons (IFNs: IFNα, IFNβ and IFNγ) cluster with interleukin 6 (IL6) by their pattern of STAT phosphorylation[3]. GPCR agonists isoproterenol (ISO) and prostaglandin E2 (PGE) cluster together due to their strong cAMP responses. 2-methylthio-ATP (2MA), platelet activating factor (PAF) and uridine diphosphate (UDP) cluster together by strong Ca^{2+} and phosphoprotein responses[4,5]. Other GPCR agonists, lysophosphatidic acid (LPA) and complement C5A, cluster with the tyrosine kinase receptor agonist macrophage colony stimulating factor (MCF). In general, the single ligand matrix shows excellent consistency with known signalling mechanisms and classifies ligands into functional groups based on characteristic ligand signature responses — a finding that provides confidence in the analytic method for assembly of disparate experimental data into a single output response profile.

The double ligand screen

To evaluate cross-talk between pathways, the AfCS also carried out the so-called 'double-ligand' screen. This experiment was designed to measure output responses for all ligands applied both singly and in pairwise combinations in matched experiments (231 combinations for 21 ligands). If two ligands act independently to alter any particular output variable, then the response to their combined application is expected to be the additive effect of applying them individually. If the combined application produces a value that is different from that expected from addition of their individual applications, then the two ligands interact by that output variable and to the extent measured by the difference. Appropriately weighted for propagated errors of measurement, this 'non-additivity' (ΔΔZ; see Methods) is the quantitative measure of cross-talk between a pair of transduction events. It is worth noting that this type of analysis of cross-talk can detect interactions between signalling pathways, but remains largely unbiased with regard to the underlying molecular mechanisms. Indeed, cross-talk may be achieved through multiple mechanisms ranging from direct communication between intracellular pathways to more indirect feedback processes such as autocrine signalling. Regardless of mechanism, all of these processes contribute to the complexity of unique signalling states in cells and therefore fall into the sphere of interest of the double-ligand screen experiment.

Examples of non-additivity between ligand responses in RAW cells are shown (Fig. 2). Each panel indicates the experimentally observed effects on one variable of a pair of ligands applied either individually (in black) or together (in red). The curve in blue represents the signal expected for the combined addition of the two ligands if they act independently; thus, the difference between the red and blue curves indicates the degree of non-additivity. C5A and UDP both mobilize Ca^{2+}, but the combined effect of the two is greater than that expected for their independent action at the peak of the calcium transient (Fig. 2a). Thus, C5A and UDP show synergy in signalling — one manifestation of cross-talk. ISO elevates intracellular cAMP markedly, whereas sphingosine-1-phosphate (S1P) does not (Fig. 2b). However, ISO and S1P

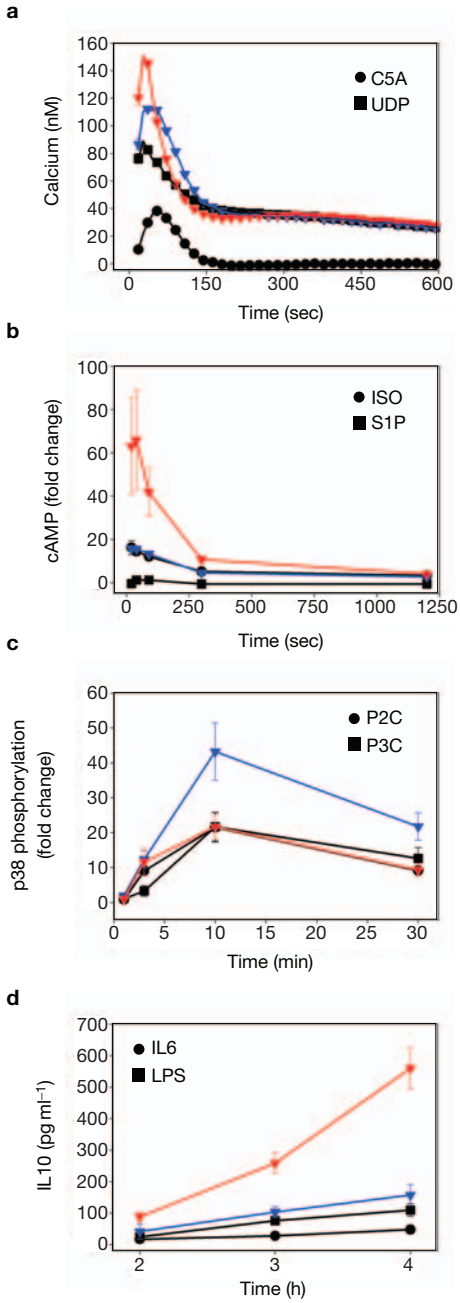

Figure 2 Non-additivity between pairs of ligands applied to RAW 264.7 cells in all four experimental assays. Each panel shows the effects of two ligands applied individually (black; see legend for ligands) or applied together (red). The calculated additive response for independent simultaneous action of the two ligands is shown in blue. The difference between the observed effect of combined addition of two ligands (the red curve) and the expected effect in the case that the ligands act independently (blue curve) is the degree to which the two ligands interact. Note that the interaction could be either positive (**a**, **b**, **d**) or negative (**c**). Error bars in all plots represent standard error of mean (n = 3–7 depending on assay). In panel **a**, symbols are shown every 10 data points.

synergize to produce a much greater than expected effect in the early phase of cAMP production. P2C and P3C both stimulate p38 MAPK phosphorylation, but the effect of the simultaneous addition of the two produces the same level of p38 phosphorylation as each ligand applied alone (Fig. 2c), suggesting saturation of a common upstream signalling component, another manifestation of cross-talk. Finally, IL6 and LPS alone both induce IL10 production, but show synergistic secretion of IL10 when combined (Fig. 2d).

Because of its size, the complete double ligand screen for all 231 ligand pairs in the RAW 264.7 cell is provided as supplementary information (see Supplementary Information, Fig. 2). Fig. 3 shows a subset of these data that allow validation of the analytic methods against known mechanisms of cross-talk and that demonstrate novel predictions. The data are shown as a matrix of ΔΔZ interaction scores for many pairs of ligands (rows) for all experimental variables (columns). Thus, each pixel indicates the degree of non-additivity for one ligand pair in one experimental measurement. For clarity, we have numbered pixels in Fig. 3 by order of presentation below. Note that most numbers highlight multiple pixels.

Interactions between all pairs of TLR ligands show systematic less-than-additive effects on many cytokines and on components of MAPK, PI(3)K and NF-κB pathways (Fig. 3a), consistent with known mechanisms of stimulation and saturation of known pathways[6,7]. As expected, TLR ligands also cooperatively interact with IFNγ and IFNβ[8–10], giving greater-than-additive IL6 and RANTES production (1). The LPS–IFNβ synergism is more muted (1), which may be accounted for by autocrine effects of LPS-induced IFNβ production that blunt the response to exogenously added interferon[11]. Interestingly, IFNβ–TLR but not IFNγ–TLR combinations show synergistic IL10 production (2) consistent with the notion that Type I IFNs selectively promote the anti-inflammatory actions of macrophages[12]. Moreover, consistent with its close clustering with the Type I IFNs in the single ligand screen (Fig. 1) and its anti-inflammatory action[13], IL6 also interacts with TLRs to stimulate IL10 production (3) and to suppress TNFα release (3). All IFN–TLR and TLR–IL6 combinations show reduced STAT1 and STAT3 phosphorylation at 30 min (4, 5), a result consistent with findings that TLR signalling leads to delayed inhibition of select cytokine signalling through production of suppressors of cytokine signalling (SOCS) proteins[14,15].

ISO and PGE decreased the production of TLR-induced cytokines MIP1α and TNFα (6), corroborating a known ISO-mediated decrease of LPS-induced TNFα production[16]. Interestingly, these ligand combinations also show increased GCSF and IL10 production (7), supporting the general notion that GPCR signalling through Gαs counteracts the TLR-mediated inflammatory response[17–19]. A specific interaction was observed for PGE and the TLR ligand P3C in synergistic IL6 production (8); this interaction has been previously described and it is argued that the suppression of TNFα production is in part mediated by increased IL6 production[20]. In summary, analysis of the ΔΔZ matrix demonstrates strong consistency with available knowledge of interactions between signalling pathways.

New interaction mechanisms derived from the ΔΔZ interaction matrix

The ΔΔZ interaction matrix also demonstrates novel interactions between signalling pathways. Consider the interactions between ligands inducing cAMP production (ISO, PGE) and Ca^{2+}-mobilizing ligands (2MA, C5A, LPA, PAF and UDP; Fig. 3). Nearly all combinations of these ligand groups cause synergistic increases in cAMP (9) coupled with synergistic inhibition of Ca^{2+} mobilization (10). These data strongly suggest a general mutual feedback interaction between these second messenger systems in RAW 264.7 cells in which receptor-stimulated Ca^{2+}

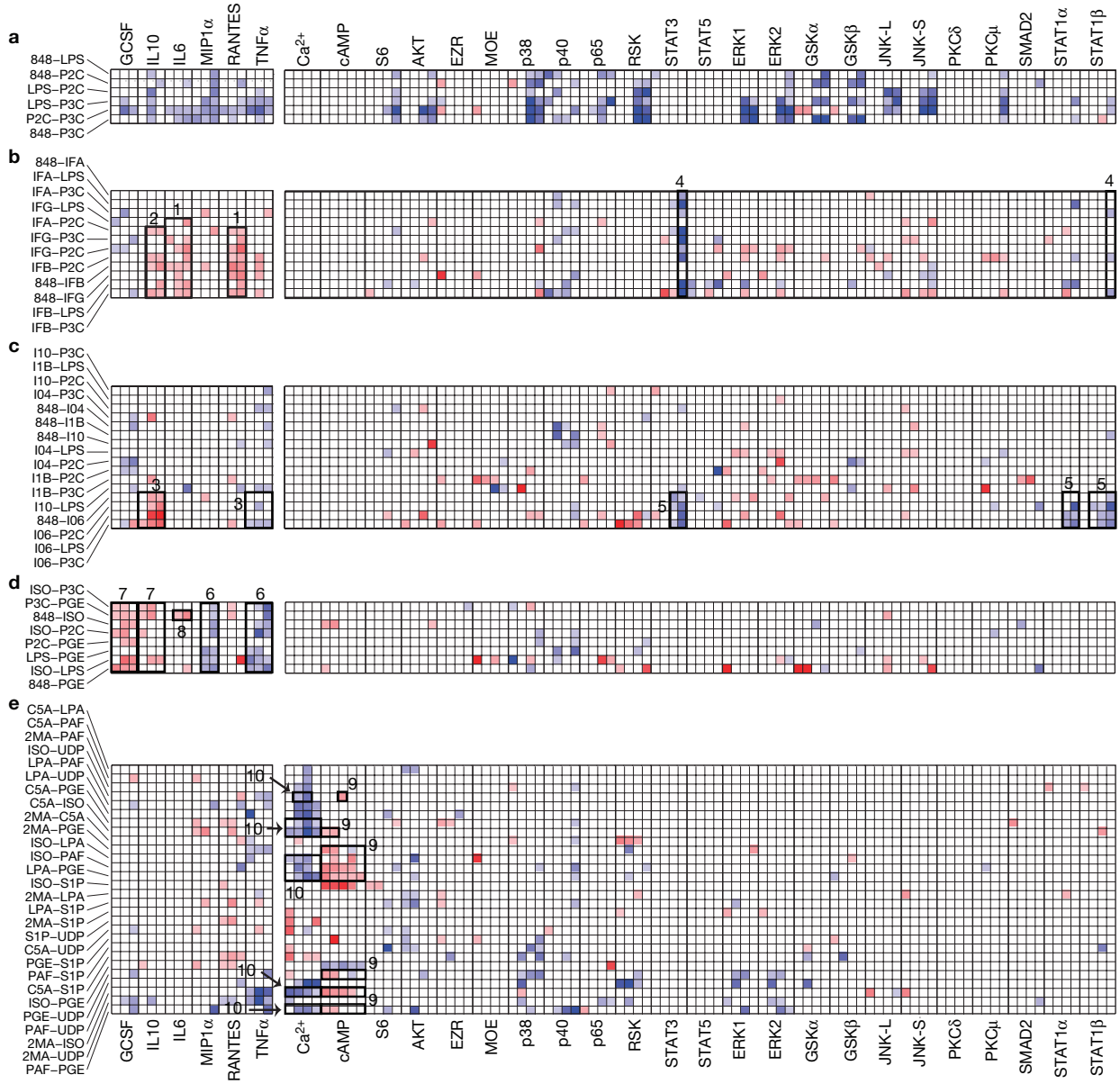

Figure 3 A subset of the double ligand screen in RAW 264.7 cells. The matrix shows the interactions between many ligand pairs (rows) for all experimental measurements (columns). The interaction is measured in ΔΔZ scores, which quantitatively report the non-additivity of responses to a pair of ligands (see text) in dimensionless units. The matrix is divided by receptor classes: **a**, TLR–TLR combinations; **b**, interferon–TLR combinations; **c**, cytokine–TLR combinations; **d**, GPCR–TLR combinations; and **e**, GPCR–GPCR combinations. Specific interactions discussed in the text are highlighted in black boxes and numbered according to the order of discussion in the text. Note that most numbers highlight multiple pixels. The colour scale for ΔΔZ ranges from – 5σ (blue) to + 5σ (red), with all insignificant values within ± 1σ in white.

elevation potentiates cAMP production, and cAMP in turn antagonizes Ca^{2+} mobilization. No single ligand or single perturbation analysis could have revealed this process as it is fundamentally defined by the cooperative interaction between two active signalling pathways. Thus it is only revealed in the double ligand experiment. We use the term 'interaction agent' to describe a signalling circuit that is uniquely involved in the coupling of distinct signalling pathways. By providing context dependence of signalling events and increasing the number of irreducible signalling states, interaction agents increase the total processing complexity of the signalling network in cells.

To better understand the Ca^{2+}–cAMP interaction mechanism, we examined how the non-additivity between Ca^{2+} and cAMP signalling is affected by perturbation of intracellular calcium and cAMP levels (Fig. 4). ISO-mediated cAMP increase is potentiated by the presence of UDP, a Ca^{2+}-stimulating agonist (Fig. 4a; compare dark grey and black bars). This synergy persists for approximately 90 s, consistent with the time course of the UDP-dependent calcium response in RAW 264.7 cells. Pretreatment of cells with 1 μM thapsigargin, an agent that depletes intracellular stores of Ca^{2+} by inhibiting re-uptake through Ca^{2+}-ATPases, partially inhibited the synergy (Fig. 4a, yellow bars), supporting a causal link between Ca^{2+} mobilization and potentiation of cAMP production by ISO. Pretreatment of cells with 2 mM extracellular EGTA, a calcium chelator, did not inhibit the synergy at early times (20 s), but inhibited at later times (40 and 90 s), consistent with

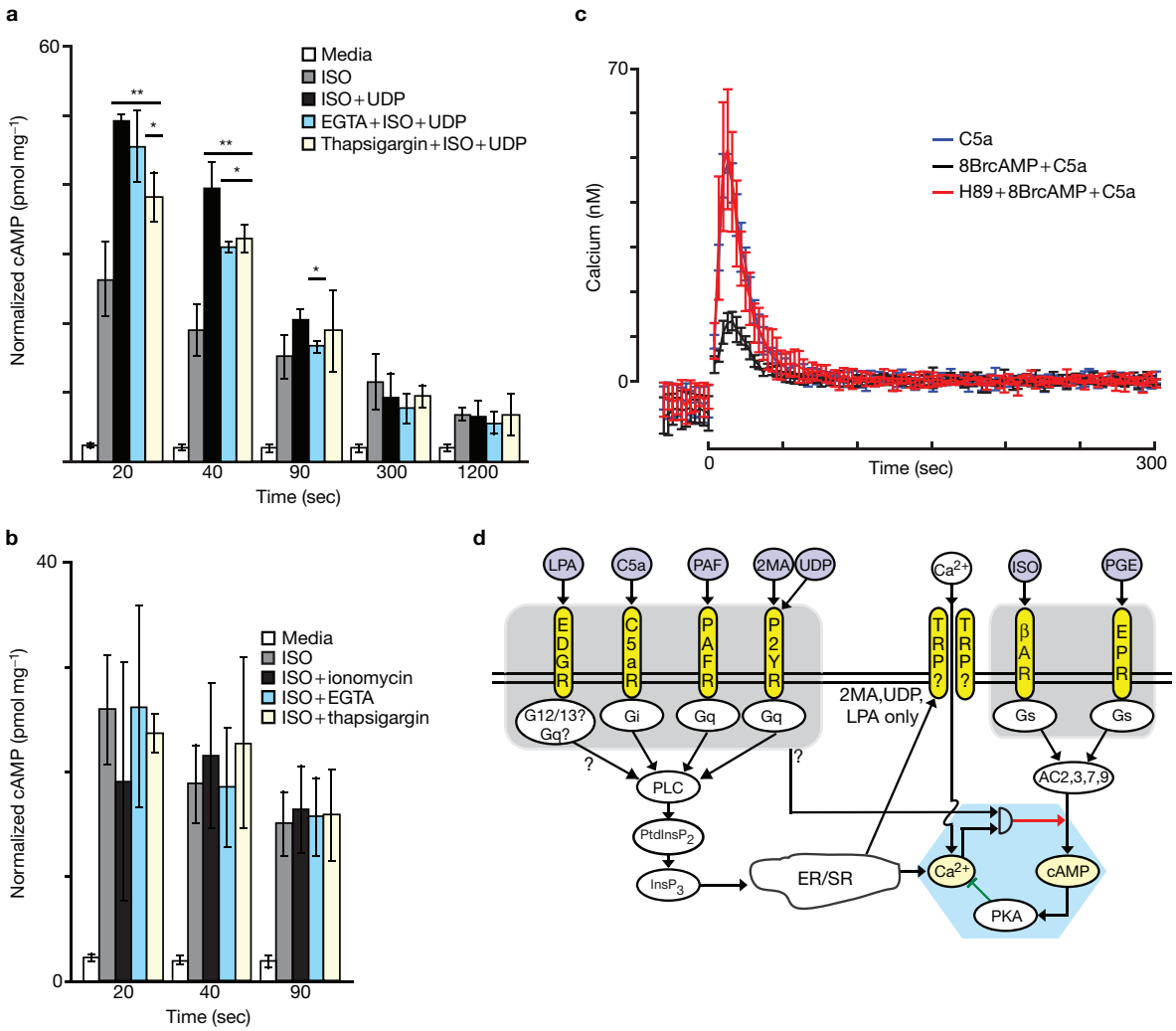

Figure 4 Testing the predicted interaction agent between calcium and cAMP. (**a**) Histograms represent normalized cAMP responses (mean ± s.d., n = 3) to stimulations with ISO (dark grey), ISO + UDP (black), and to ISO + UDP after pretreatment with EGTA (light blue) or thapsigargin (light yellow). Responses that were statistically different (P <0.05) from ISO and ISO + UDP are indicated (double and single asterisk, respectively). All responses were statistically significant from media alone (white). (**b**) Normalized cAMP responses (mean ± s.d., n = 3) to stimulation with ISO alone (dark grey) or following pretreatment with either ionomycin (black), EGTA (light blue) or thapsigargin (light yellow) are shown. Responses on pretreatment were not statistically different from ISO alone. All treatments were significantly elevated over responses to media alone (white). (**c**) The time course of intracellular calcium levels in response to C5a (blue, mean ± s.d., n = 6,) was significantly inhibited by 8BrcAMP (black). Pretreatment with H89 (red) blocked the inhibitory influence of 8BrcAMP. (**d**) A schematic representation of the interaction agent mediating cross-talk between Ca^{2+} and cAMP. GPCR ligands (blue ovals) act on cognate receptors (dark yellow ovals; grouped by Ca^{2+} and cAMP stimulators) and activate appropriate Gα-subunits and subsequent signalling cascades (all signalling shown as black arrows). A receptor-dependent Ca^{2+} increase (symbolized as a logical AND gate) synergizes (red arrow) with the Gαs-stimulated production of cAMP. Feedback from cAMP inhibits levels of intracellular calcium by a PKA-dependent mechanism (green line). An interaction agent summarizing and defining the conditional cross-talk between Ca^{2+} and cAMP is highlighted by a blue hexagon.

the observation that UDP-dependent intracellular calcium mobilization comes in two phases — initial release from thapsigargin-sensitive intracellular stores followed by influx through plasma membrane calcium channels (Fig. 4a, blue bars). Pretreatment of cells with thapsigargin, EGTA or 2 μM ionomycin (a calcium ionophore that raises intracellular calcium to an extent similar to that induced by UDP) also had no effect on ISO-mediated cAMP production (Fig. 4b; light yellow, blue and black bars, respectively). Thus, calcium mobilization alone, in the absence of receptor stimulation, is insufficient to support synergistic control of ISO signalling. Taken together, these results indicate that ISO-mediated cAMP production is specifically upregulated by receptor-mediated calcium mobilization.

The mechanisms by which increase in cAMP production leads to suppression of receptor-mediated intracellular calcium mobilization were further explored. The GPCR agonist C5a induces a large transient elevation in intracellular calcium (Fig. 4c, blue), but in cells pretreated with a cell-permeable, non-hydrolysable analogue of cAMP (8BrcAMP, 2 mM), this response was significantly attenuated (Fig. 4c, black). Interestingly, the effect of 8BrcAMP could be completely blocked by the pretreatment of cells with 12.5 μM H89, a selective inhibitor of protein kinase A (PKA; Fig. 4c, red). These data argue that cAMP-mediated control of calcium signalling operates through a PKA-dependent process.

Taken together, these data provided an initial mechanistic model for a novel signalling circuit that represents the Ca^{2+}–cAMP interaction agent

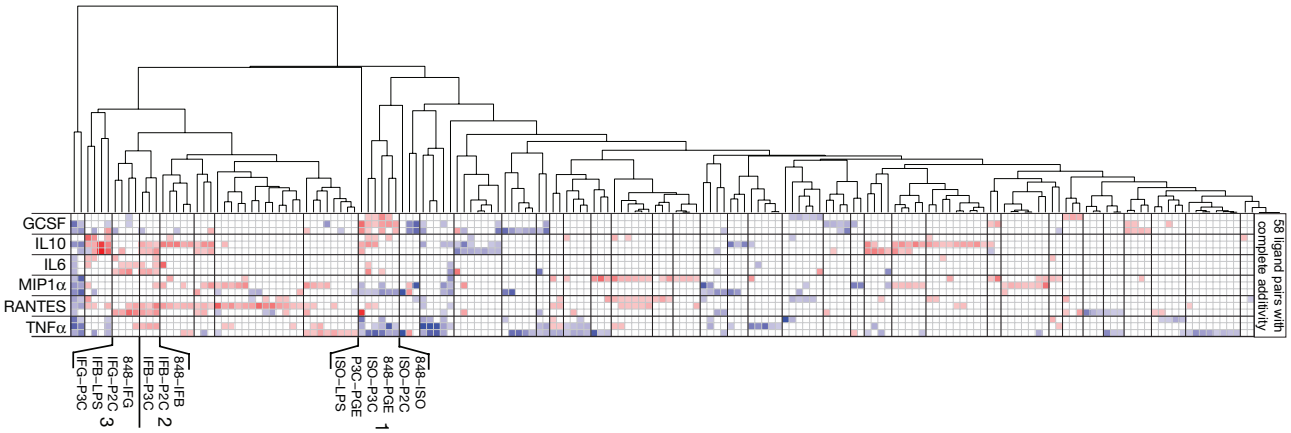

Figure 5 The complete double ligand screen in RAW 264.7 cells describing non-additivity in the secretion of cytokines in response to all 231 pairwise combinations of 22 input ligands. The matrix is hierarchically clustered, and follows the same colour scheme in Fig. 3. Ligand pairs for select clusters (labelled 1–3) are displayed (see Supplementary Information, Fig. S2 for all labels). Analysis of clustering patterns shows that the primary effect of most ligands is exerted through modulation of cytokine production as against direct control; for example, cluster 1 shows that IFNs, which do not directly stimulate significant production of cytokines (Fig. 1), are capable of significant modulation of TLR-induced cytokine release.

(Fig. 4d, blue hexagon). Receptor-mediated elevations of intracellular calcium lead to potentiation of concurrent cAMP signalling. In turn, cAMP production operates through activation of PKA to inhibit receptor mediated Ca^{2+} mobilization. Further work will be necessary to completely expose the details of operation of this circuit, but these data serve to illustrate the core concept of the interaction agent — a network of signalling reactions that are silent during single pathway signalling events, but that become active during the simultaneous activation of multiple signalling pathways and provide the capacity for context dependence of signal processing. Analysis of the ΔΔZ interaction matrix is one practical experimental approach for recognizing these interaction agents and for designing new experiments to mechanistically understand them.

A global assessment of signalling cross-talk

To examine the total density of cross-talk between signalling pathways. we performed a complete assesment of non-additive interactions for all 231 ligand pairs, focused on the six cytokines that represent the significant final outputs of RAW 264.7 cells in our screen (Fig. 5). The matrix shows the non-additivity in the production of these cytokines (rows) for all ligand pairs (columns) and is clustered so that ligand pairs displaying a similar pattern of non-additivity are grouped together. The statistical significance of clusters was assessed by comparing the clustering of the actual data with that resulting from 1000 trials of randomly scrambling the ΔΔZ matrix (see Supplementary Information, Fig. 3 and Methods). Significant clusters are indicated by bold divisions.

The data show that all of the 22 ligands that are included in this study display at least one non-additive interaction with another ligand in modulating cytokine production (Fig. 5, columns and see Supplementary Information, Fig. S2). Similarly, every cytokine is apparently subject to both synergistically-positive and synergistically-inhibitory regulation through distinct pairwise combination of ligands (Fig. 5, rows and see Supplementary Information, Fig. S2). This is true despite the fact that many of these ligands failed to show any effect on cytokine production when applied individually (for example, ISO, PGE, and TGFβ; Fig. 1). Thus we conclude that: first, interactions are many, providing a rich capacity for context dependent signalling in RAW 264.7 cells; and second, that the physiological role of most signalling pathways is not autonomous control over main cellular outputs, but is instead context-dependent regulation of a few signalling pathways that can exert direct control.

At first glance, the finding that there are many pairwise interactions between ligands suggests the possibility that a vast number of interaction agents exists, each serving to mediate the synergistic activity of unique ligand combinations. However, the clustering of the ΔΔZ matrix suggests otherwise. Though many non-additive interactions are evident, ligand pairs fall into a modest number of clusters (approximately 40) based on the pattern of non-additivity (Fig. 5). These observations lead to the hypothesis that clusters represent the convergence of signalling pathways onto a small set of interaction mechanisms that combine to yield a limited number of unique cytokine regulatory programs. For example, consider cluster 1 in Fig. 5, which comprises TLR agonists paired with the GPCR ligands ISO and PGE. Activation of TLR signalling on its own leads to strong increases in production of all the cytokines included in this analysis (Fig. 1). However, according to the clustering, the coincident activity of a GPCR that mobilizes cAMP leads to a unique cytokine expression program that could not have been predicted from knowledge of the TLR or GPCR ligand responses taken independently: GCSF, IL6, RANTES and IL10 are variously potentiated, and MIP1α and TNFα are suppressed. Note that no other cluster shows this cytokine expression program; it is a specific feature of these ligand combinations alone. These results suggest the existence of a generic interaction agent that links cAMP production to the specific modulation of TLR signalling.

To test this, we examined the effect of LPS, a TLR agonist, on production of these six cytokines with or without treatment of cells with 8BrcAMP (Fig. 6a). The data confirm that cAMP elevation is sufficient to induce the same modulation of TLR signalling to yield the same cytokine expression pattern as in the double-ligand experiment. The modulatory effects of cAMP are also demonstrated at the gene expression level (http://www.signaling-gateway.org/data/micro/cgi-bin/micro.cgi); application of LPS alone induces cytokine and other genes, ISO or PGE do little on their own, but the costimulation with either ISO plus LPS, or PGE plus LPS, leads to synergistic induction of many genes including GCSF, IL6 and IL10, and synergistic repression of genes including TNFα (Fig. 6b). These data support the model that ISO–PGE signalling modulates TLR signalling through a cAMP-dependent process that is comprised of an interaction

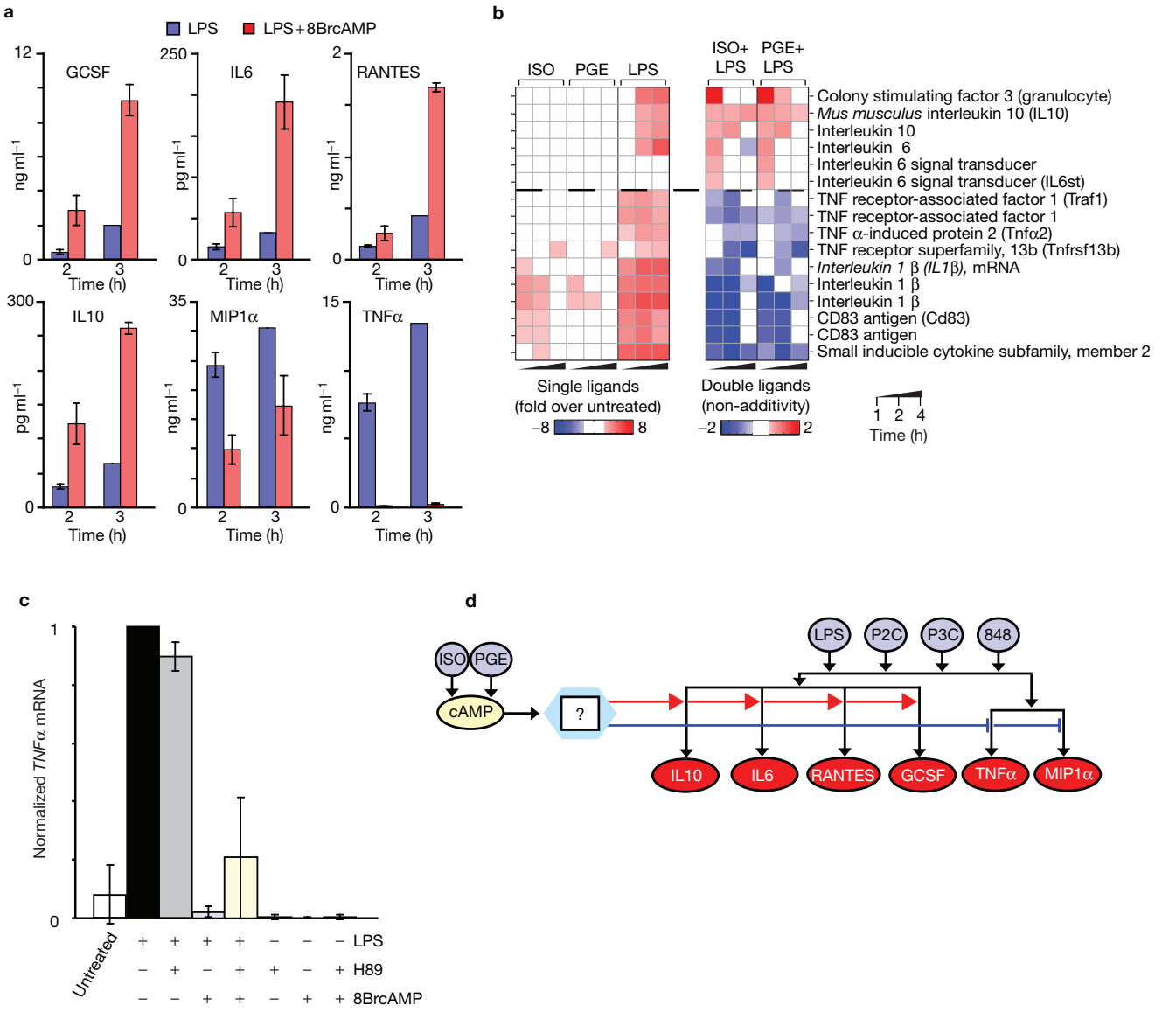

Figure 6 Testing the predicted interaction agent between Gαs–GPCRs and TLRs. (**a**) GCSF, IL6, RANTES, IL10, MIP1α and TNFα secretion at 2 and 3 h after stimulation by LPS (blue) or LPS+8BrcAMP (red; mean ± s.d., n = 2, normalized to maximum LPS response). (**b**) The regulation of 21 genes (mean fold change over responses in untreated cells) in response to stimulation by each of ISO, PGE and LPS (30 microarrays; 1, 2 and 4 h) is shown in the left panel (red pixels indicate upregulation; white pixels indicate unchanged; blue pixels indicate downregulation). Some genes have the same descriptive names but have different nucleotide sequences (systematic names) on the chip. The panel on the right shows the non-additivity of responses to the pairs of ligands ISO + LPS and PGE + LPS (red pixels indicate synergy; blue pixels indicate inhibition). Note the systematic inhibitory influence of Gαs on several members of the inflammatory cascade (for example, interleukin-1b, cd83 antigen abd mip2) that are upregulated by TLR signalling. (**c**) Levels of TNFα transcript assayed by quantitative RT–PCR 2 h after stimulation (n = 3, mean ± s.d., normalized to maximum LPS response). The response to LPS (black) is completely inhibited in the presence of 8BrcAMP (light blue). This inhibition is not mediated by PKA as H89 does not significantly reduce the inhibition of 8BrcAMP on the LPS-induced TNFα response (light yellow). Controls responses to H89 (red), 8BrcAMP (light green) and H89 + 8BrcAMP (dark yellow) are not different from untreated cells (white) at 2 h. (**d**) A schematic representation of the interaction agent mediating cross-talk between Gαs–GPCRs and TLRs. Colour convention is similar to Fig. 4d. TLR agonists induce secretion of multiple cytokines (red ovals). Stimulation of Gαs–GPCRs selectively mediates both synergy and inhibition of TLR-induced cytokine responses through an unknown interaction agent (blue hexagon), that is independent of PKA activation in the regulation of at least one cytokine.

agent — a signalling circuit that provides generic communication between these signalling pathways and that is only exposed in the coincident activity of the pathways (Fig. 6d). From a biological point of view, this interaction agent makes sense; Gαs-signalling in macrophage cells is known to attenuate the inflammatory response due to TLR activity[16,21].

To characterize possible cAMP-dependent processes that may be involved in this cross-talk, the effect of the PKA inhibitor H89 on the ability of 8BrcAMP to suppress LPS-dependent TNFα production was examined (Fig. 6c). The data show that H89 does not significantly affect the modulatory effect of cAMP on LPS signalling. Thus, at least with regard to the LPS-induced TNFα production, PKA is unlikely to be part of the cAMP-dependent modulatory cascade. These data show how the same signalling molecule (for example, cAMP) can be involved in multiple interaction agents. In this case, cAMP-dependent control of receptor-mediated Ca^{2+} mobilization occurs through a PKA-dependent process, and modulation of aspects of TLR signalling occurs through a PKA-independent process.

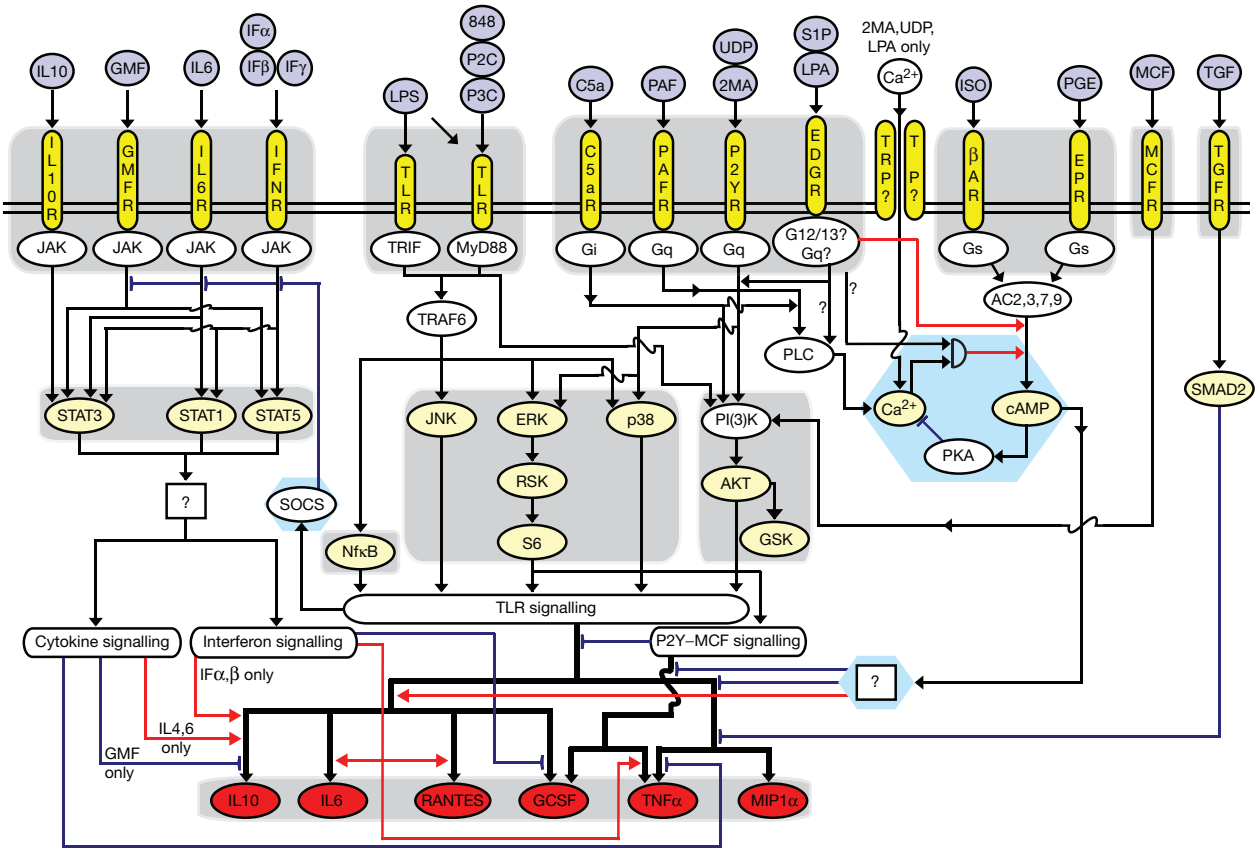

Figure 7 A schematic compilation of input–output relationships observed in the single and double-ligand screens. The representations follow previous examples (Figs 4d and 6d). Assayed parameters in the ligand screens are shown as light yellow ovals. Other known mechanisms (not assayed) are depicted as white ovals. Transcription factors (collectively described for each group of ligands, white rounded rectangles) are activated and undergo translocation (thick black lines) to produce cytokines (red ovals), the final step in the input-output relationship. Interactions from the double ligand screen are shown as coloured arrows (red arrows indicate synergistic; blue arrows indicated less than additive). For visual clarity, interactions within groups are not displayed (for example, interactions between TLRs). Three interaction agents revealed by the double ligand screen are also indicated (blue hexagons).

Other clusters in the ΔΔZ matrix also support the notion of interaction agents. For example, clusters 2 and 3 reveal systematic pairwise interactions between interferon and TLR signalling pathways with regard to production of cytokines, a finding that is consistent with many other studies[8–10]. Several mechanisms have been proposed for mediating such an interaction: first, up-regulation of TLRs by IFN signalling[22–24]; second, potentiation of NF-κB[25] and/or ERK and STAT[26] signalling pathways; and third, induction of the SOCS proteins[27,28], a family of regulatory molecules that are induced by TLR signalling and act to modulate JAK–STAT signalling such as through IFNs[14,15]. Interestingly, the clustering pattern demonstrates similarities and difference between IFNβ and IFNγ signalling in RAW 264.7 cells; both IFNβ and IFNγ potentiate the production of IL-6 and RANTES by TLR signalling, but differ in that IFNβ alone synergistically enhances IL-10 production, consistent with the known anti-inflammatory role specific for Type I interferons[29].

Based on these results, we propose that clustering of ligand interactions based on cytokine production originates from the existence of a limited set of interaction agents that provide the capacity to integrate specific signalling pathways to yield unique output responses. The relatively small number of clusters suggests the possibility that most of the combinatorial complexity of signalling may be accounted for by the convergence of signalling cascades on a small number of molecular mechanisms.

DISCUSSION

The work presented here provides initial insights into the architecture of the intracellular signalling machinery in the RAW 264.7 cells and provides important direction for further experimentation. A simplified picture (Fig. 7) of the signalling network that emerges from the single and double ligand screens serves to illustrate the basic results. Ligands taken individually cluster into specific response classes that reflect commonality in their early transduction mechanisms but fails to explain their physiological contribution to information processing. Taken in pairwise combinations, ligands begin to reveal their context-dependent roles in modulating final cellular outputs; indeed, the data suggest that the primary activity of many input ligands is modulation of other signalling systems rather than direct control over cellular outputs. The density of cross-talk demonstrates substantial capacity for encoding combinatorial complexity in input stimuli, but the clustering of non-additive response patterns places significant constraints on the mechanistic complexity of ligand interactions. We suggest that the topology of the signalling network in the RAW 264.7 cell is composed of modular transduction units representing the core transduction machinery downstream of specific receptor classes linked by a limited set of interaction agents whose number and promiscuity ultimately determine the processing complexity of the cell. The availability of an open access, high quality dataset of ligand responses, and the interactions between them in one cell type, should enable the signalling community to systematically test this hypothesis.

METHODS

Single-ligand responses. An error model was constructed for each data variable by collecting several datasets for mock-stimulated cells, which were defined as the reference (or basal) state. This provided a mean value and an expected variance for each variable with no applied stimulus. Each data variable collected on ligand stimulation was then expressed as the number of standard deviations removed from the error model (for example, the *Z*-score). Thus, for ligand *i* generating a value of a_i for the experimental variable *x*, the transformed representation of the value is given by:

$$Z_i^x = \frac{a_i - \overline{a_{basal}}}{\sigma_{basal}}$$

where Z_i^X is the significance of observing a_i given the error model. Multiple repeats of applying ligand *i* produced a distribution of *Z*-scores for variable *x*; thus, the raw data variable is transformed into a mean *Z*-score with errors, and these are used to derive parameters for ligand similarity and interaction.

Double-ligand screen. This screen was used to identify cross-talk between ligands. Quantitatively, we define the 'interaction' of two ligands (1 and 2) on experiment variable *x* as:

$$\Delta\Delta Z_{1,2}^x = \frac{Z_{1,2}^x - (Z_1^x + Z_2^x)}{\sqrt{\sigma_{1,2}^2 + \sigma_{1+2}^2}}$$

where the difference between the observed effect of applying both ligands ($Z_{1,2}^X$) and the expected effect if they act independently ($Z_1^X + Z_2^X$) is weighted for the propagated errors of measurement. We note that $\Delta\Delta Z_{1,2}^X$ is not merely the difference between two ligand responses; it is a new parameter that gives the degree to which two ligands cooperatively determine each experiment variable. This interaction could arise from many sources and by itself says little about the underlying molecular mechanism. Nevertheless, it indicates complexity as it detects the context-dependence of specific output variables in the transduction of stimuli.

Clustering methods. All clustering was performed using implementations of hierarchical clustering in MATLAB (The Mathworks, Natick, MA). Distance calculations were made using the cityblock metric and linkages were established using the complete linkage method. Inconsistency coefficients[30] were calculated for each node in a dendrogram to rank the significance of clustering for the ΔΔZ matrix (Fig. 5). Briefly, an inconsistency coefficient of zero places every leaf node in a dendrogram in its own separate cluster while at the maximum inconsistency score all leaf nodes comprise a single cluster. To determine a threshold inconsistency score for partitioning leaf nodes in the ΔΔZ matrix into an optimal number of clusters the inconsistency scores for clustering the matrix were calculated following 1,000 trials of random permutation of the columns of the matrix. This randomization scrambled any similarities in patterns of non-additivity between ligand pairs; thus clustering in the randomized matrices is insignificant. A comparison of the number of clusters generated as a function of the inconsistency coefficient for the ΔΔZ matrix and the randomized trials provides the threshold value for cluster significance (see Supplementary Information, Fig. S3).

Experimental methods. Detailed protocols for the ligand screens developed by the AfCS are available online (http://www.signaling-gateway.org/data/ProtocolLinks.html). Brief summaries of key procedures are described in the Supplementary Methods.

cAMP assays. Intracellular cAMP levels were assayed identical to procedures in the ligand screen (AfCS Procedure Protocol ID: PP00000175) using an enzyme-linked immunoassay system (cAMP Biotrack EIA; Amersham Biosciences, Piscataway, NJ). Cells were stimulated with ISO (50 nM, Sigma-Aldrich, St Louis, MO), UDP (25 μM, Sigma-Aldrich) or both. Stimulations with combinations of ISO + UDP were performed in the presence (pretreatment for 5 min) and absence of thapsigargin (1 μM, Calbiochem, La Jolla, CA) or EGTA (2 mM, Sigma-Aldrich). Reactions were stopped at the times indicated after addition of stimulus and cAMP content was determined. To reduce day-to-day variability, cAMP levels on each day were normalized by area normalization of the ISO + UDP response for that experiment.

Calcium assays. Assay of intracellular calcium followed the same procedure as the ligand screen experiments (AfCS Procedure Protocol ID: PP00000176). Cells were stimulated with C5a (100 nM, Calbiochem) in the absence and presence of 8BrcAMP (2 mM, Sigma-Aldrich), H89 (12.5 μM, Biomol, Plymouth Meeting, PA) or both. Cells were pretreated with 8BrcAMP and H89 5 min and 10 min before C5a stimulation, respectively. Data were normalized to the peak of the C5a response for comparison.

Cytokine assays. Assay of cytokine secretion followed the same procedure as the ligand screen experiments (AfCS Procedure Protocol ID PP00000209, -221, -223). Cells were stimulated with LPS (100 ng ml^{-1}, Sigma-Aldrich; all LPS treatments were made with added LBP 250 pM, R&D Systems, Minneapolis, MN) or with a combination of LPS and 8BrcAMP (1 mM). Supernatants were collected at 2 and 3 h after initiation of stimulation and assayed for cytokine content. Data were normalized to the maximum secretion of each cytokine in response to LPS treatment alone. For estimation of cytokine mRNA levels, cells treated as above were lysed for mRNA extraction (RNeasy plus mini kit, Qiagen, Valencia, CA) and subsequent cDNA synthesis (Copy kit, Invitrogen, Carlsbad, CA) that was used as template for quantitative RT–PCR reactions. Primers for the TNFα gene were designed using Primer3 (ref. 31) based on design constraints of melting temperatures >60 °C, GC content >50% and size <30 base pairs (bp), with the final product spanning at least two introns (275 bp). The following primers were used: 2R-TNFα, TACGACGTGGGCTACAGGCTTG; 2F-TNFα, GAAAGCATGATCCGCGACGTGGA. A reference gene (18S) and reference cDNA synthesized from RNA isolated from total spleen (a kind gift from J. Lee, UTSWMC) were used for normalization for each reaction. Day-to-day variability between experiments was reduced by normalizing to maximum LPS response.

Microarray experiments. Publicly available AfCS microarray data was used to examine interactions between ligands. Data from 30 AfCS microarray experiments (five ligands; ISO, PGE, LPS, ISO + LPS and PGE + LPS at three timepoints (1, 2 and 4 h), repeated twice; see Supplementary Information, Table S1 for ligand details) were downloaded and analyzed using custom scripts written in MATLAB (R14, The Mathworks).

Note: Supplementary Information is available on the Nature Cell Biology website.

ACKNOWLEDGEMENTS

We are indebted to the many individuals from several academic institutes that are members of the AfCS scientific team for data collection, for database construction and for providing general help and advice. this work would not have been possible without the transparent and efficient public access to raw experimental data supported by the AfCS effort. We also thank members of the AfCS steering committee and the Ranganathan lab for discussion and critical reading of the manuscript. Work on this project was supported by contributions from public and private sources, including the NIGMS Glue Grant Initiative (U54 GM062114). A complete listing of the AfCS sponsors can be found at http://www.signalling-gateway.org/aboutus/sponsors.html. R.R. acknowledges support from the Mallinckrodt Scholar award, the Keck Future Initiatives award and the Robert A. Welch Foundation, and is an investigator of the Howard Hughes Medical Institute. P.C.S. acknowledges support from the Robert A. Welch Foundation and is the Alfred and Mabel Gilman Chair in molecular pharmacology.

COMPETING FINANCIAL INTERESTS

The authors declare that they have no competing financial interests.

Published online at http://www.nature.com/naturecellbiology/
Reprints and permissions information is available online at http://npg.nature.com/reprintsandpermissions/

1. Gilman, A. G. *et al.* Overview of the Alliance for Cellular Signaling. *Nature* **420,** 703–706 (2002).
2. Akira, S., Yamamoto, M. & Takeda, K. Role of adapters in Toll-like receptor signalling. *Biochem. Soc. Trans.* **31,** 637–642 (2003).
3. Ihle, J. N. Cytokine receptor signalling. *Nature* **377,** 591–594 (1995).
4. Chen, Z. P., Levy, A. & Lightman, S. L. Nucleotides as extracellular signalling molecules. *J. Neuroendocrinol.* **7,** 83–96 (1995).
5. Chen, L. W., Lin, M. W. & Hsu, C. M. Different pathways leading to activation of extracellular signal-regulated kinase and p38 MAP kinase by formyl-methionyl-leucyl-phenylalanine or platelet activating factor in human neutrophils. *J. Biomed. Sci.* **12,** 311–319 (2005).
6. Sato, S. *et al.* Synergy and cross-tolerance between toll-like receptor (TLR) 2- and TLR4-mediated signaling pathways. *J. Immunol.* **165,** 7096–7101 (2000).

7. Medvedev, A. E., Kopydlowski, K. M. & Vogel, S. N. Inhibition of lipopolysaccharide-induced signal transduction in endotoxin-tolerized mouse macrophages: dysregulation of cytokine, chemokine, and toll-like receptor 2 and 4 gene expression. *J. Immunol.* **164,** 5564–5574 (2000).
8. Hemmi, H. *et al.* The roles of two IκB kinase-related kinases in lipopolysaccharide and double stranded RNA signaling and viral infection. *J. Exp. Med.* **199,** 1641–1650 (2004).
9. Hausler, K. G. *et al.* InterferonK differentially modulates the release of cytokines and chemokines in lipopolysaccharide- and pneumococcal cell wall-stimulated mouse microglia and macrophages. *Eur. J. Neurosci.* **16,** 2113–2122 (2002).
10. Yamamoto, M. *et al.* Cutting edge: a novel Toll/IL-1 receptor domain-containing adapter that preferentially activates the IFN-β promoter in the Toll-like receptor signaling. *J. Immunol.* **169,** 6668–6672 (2002).
11. Gessani, S., Belardelli, F., Pecorelli, A., Puddu, P. & Baglioni, C. Bacterial lipopolysaccharide and γ-interferon induce transcription of β-interferon mRNA and interferon secretion in murine macrophages. *J. Virol.* **63,** 2785–2789 (1989).
12. Tilg, H. & Kaser, A. Type I interferons and their therapeutic role in Th2-regulated inflammatory disorders. *Expert Opin. Biol. Ther.* **4,** 469–481 (2004).
13. Aderka, D., Le, J. & Vilcek, J. IL-6 inhibits lipopolysaccharide-induced tumor necrosis factor production in cultured human monocytes, U937 cells, and in mice. *J. Immunol.* **143,** 3517–3523 (1989).
14. Heeg, K. & Dalpke, A. TLR-induced negative regulatory circuits: role of suppressor of cytokine signaling (SOCS) proteins in innate immunity. *Vaccine* **21,** S61–S67 (2003).
15. Niemand, C. *et al.* Activation of STAT3 by IL-6 and IL-10 in primary human macrophages is differentially modulated by suppressor of cytokine signaling 3. *J. Immunol.* **170,** 3263–3272 (2003).
16. Zhang, H. *et al.* Effect of adrenoreceptors on endotoxin-induced cytokines and lipid peroxidation in lung explants. *Am. J. Respir. Crit. Care Med.* **160,** 1703–1710 (1999).
17. Lukashev, D., Ohta, A., Apasov, S., Chen, J. F. & Sitkovsky, M. Cutting edge: Physiologic attenuation of proinflammatory transcription by the Gs protein-coupled A2A adenosine receptor *in vivo*. *J. Immunol.* **173,** 21–24 (2004).
18. O'Donnell, P. M. & Taffet, S. M. The proximal promoter region is essential for lipopolysaccharide induction and cyclic AMP inhibition of mouse tumor necrosis factor-α. *J. Interferon Cytokine Res.* **22,** 539–548 (2002).
19. Hareng, L., Meergans, T., von Aulock, S., Volk, H. D. & Hartung, T. Cyclic AMP increases endogenous granulocyte colony-stimulating factor formation in monocytes and THP-1 macrophages despite attenuated TNF-α formation. *Eur. J. Immunol.* **33,** 2287–2296 (2003).
20. Akaogi, J. *et al.* Prostaglandin E2 receptors EP2 and EP4 are up-regulated in peritoneal macrophages and joints of pristane-treated mice and modulate TNF-α and IL-6 production. *J. Leukoc. Biol.* **76,** 227–236 (2004).
21. Farmer, P. & Pugin, J. β-adrenergic agonists exert their 'anti-inflammatory' effects in monocytic cells through the IκB/NF-κB pathway. *Am. J. Physiol. Lung Cell Mol. Physiol.* **279,** L675–L682 (2000).
22. Nansen, A. & Randrup Thomsen, A. Viral infection causes rapid sensitization to lipopolysaccharide: central role of IFN-αβ. *J. Immunol.* **166,** 982–988 (2001).
23. Durbin, J. *et al.* The role of STAT1 in viral sensitization to LPS. *J. Endotoxin. Res.* **9,** 313–316 (2003).
24. Hertzog, P. J., O'Neill, L. A. & Hamilton, J. A. The interferon in TLR signaling: more than just antiviral. *Trends Immunol.* **24,** 534–539 (2003).
25. Harada, K., Isse, K. & Nakanuma, Y. Interferon gamma accelerates NF-κB activation of biliary epithelial cells induced by Toll-like receptor and ligand interaction. *J. Clin. Pathol.* **59,** 184–190 (2006).
26. Zhao, J. *et al.* IRF-8/ICSBP is involved in TLR signaling and contributes to the cross talk between TLR and IFN-γ signaling pathways. *J. Biol. Chem.* **281,** 10073–10080 (2006).
27. Baetz, A., Frey, M., Heeg, K. & Dalpke, A. H. Suppressor of cytokine signaling (SOCS) proteins indirectly regulate toll-like receptor signaling in innate immune cells. *J. Biol. Chem.* **279,** 54708–54715 (2004).
28. Dalpke, A. H. & Heeg, K. Synergistic and antagonistic interactions between LPS and superantigens. *J. Endotoxin Res.* **9,** 51–54 (2003).
29. Vandeusen, J. B. *et al.* STAT-1-mediated repression of monocyte interleukin-10 gene expression *in vivo*. *Eur. J. Immunol.* **36,** 623–630 (2006).
30. Mojena, R. Hierarchical grouping methods and stopping rules: An evaluation. *Computer J.* **20,** 359–363 (1977).
31. Rozen, S. & Skaletsky, H. Primer3 on the WWW for general users and for biologist programmers. *Methods Mol. Biol.* **132,** 365–386 (2000).

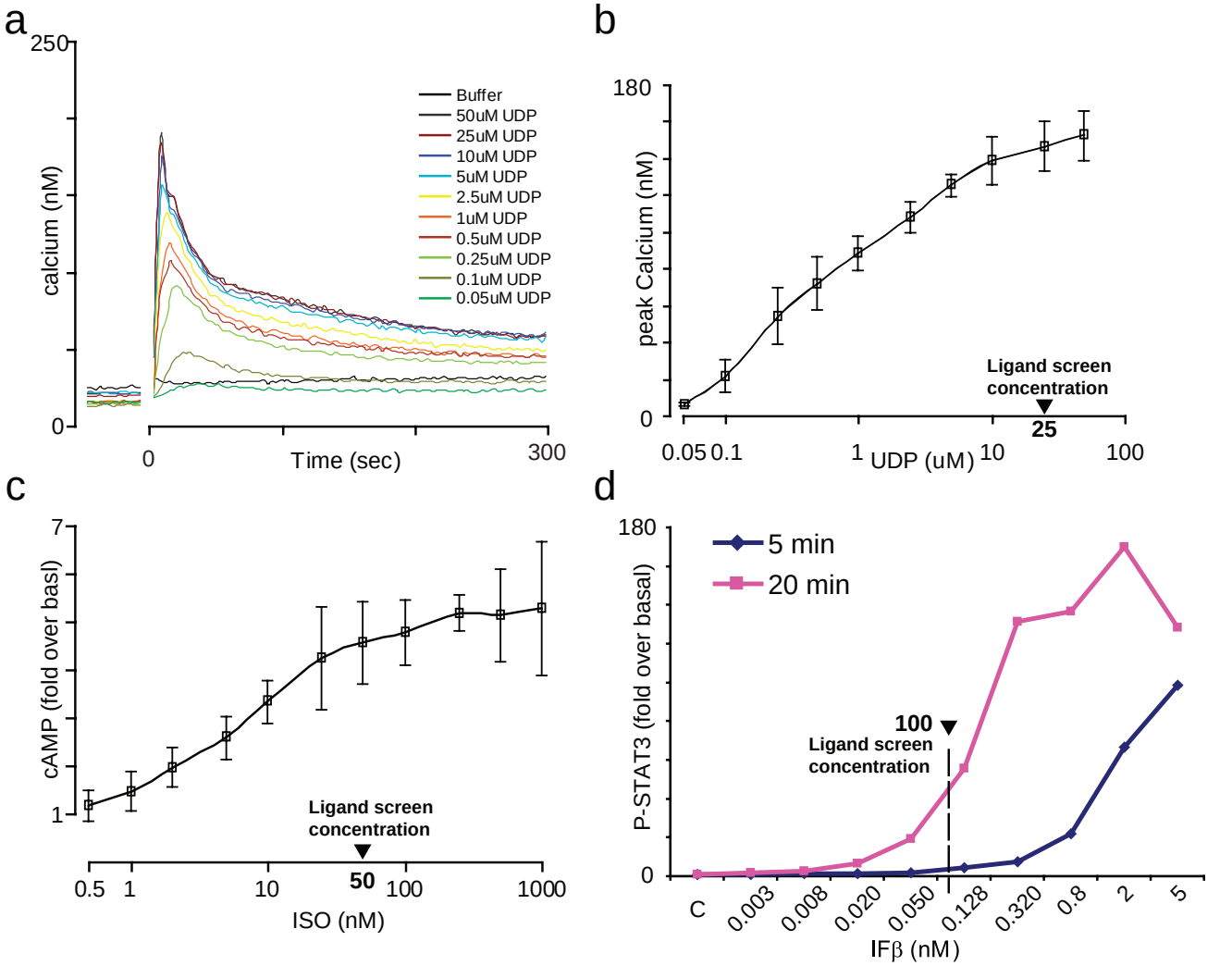

Figure S1 Selection of final ligand concentrations for the single and double ligands screens from dose-response curves. Each ligand had to induce a response in at least one assay – calcium, cAMP, phosphorylation of proteins or cytokine secretion. **a.** Concentrations of UDP at or beyond a threshold (25μM, lowest red trace) resulted in the largest average calcium response of all ligands tested, with classic calcium profiles characterized by a rapid initial transient and a sustained plateau phase lasting beyond 5 minutes. Increases in UDP concentration resulted in monotonically increasing peak amplitudes and faster rise times. **b.** The dose response curve for peak calcium responses to varying UDP concentrations from **a.** A continuously increasing trend is clearly visible with no sign of saturation. The final concentration of UDP selected for the ligand screens (25μM) is indicated (black arrowhead). **c.** cAMP production in response to increasing concentrations of ISO curve display a sigmoidal response saturating around 500 nM. The concentration of ISO used in the ligand screens (50nM) is indicated (black arrowhead). **d.** Phosphorylation of the protein STAT3 in response to increasing concentrations of IFβ were measured at multiple times (shown 5, 20 minutes). The final concentration of IFβ used in the ligand screens (100pM) is indicated (black arrowhead).

Supplementary Figure 2
Natarajan et al.

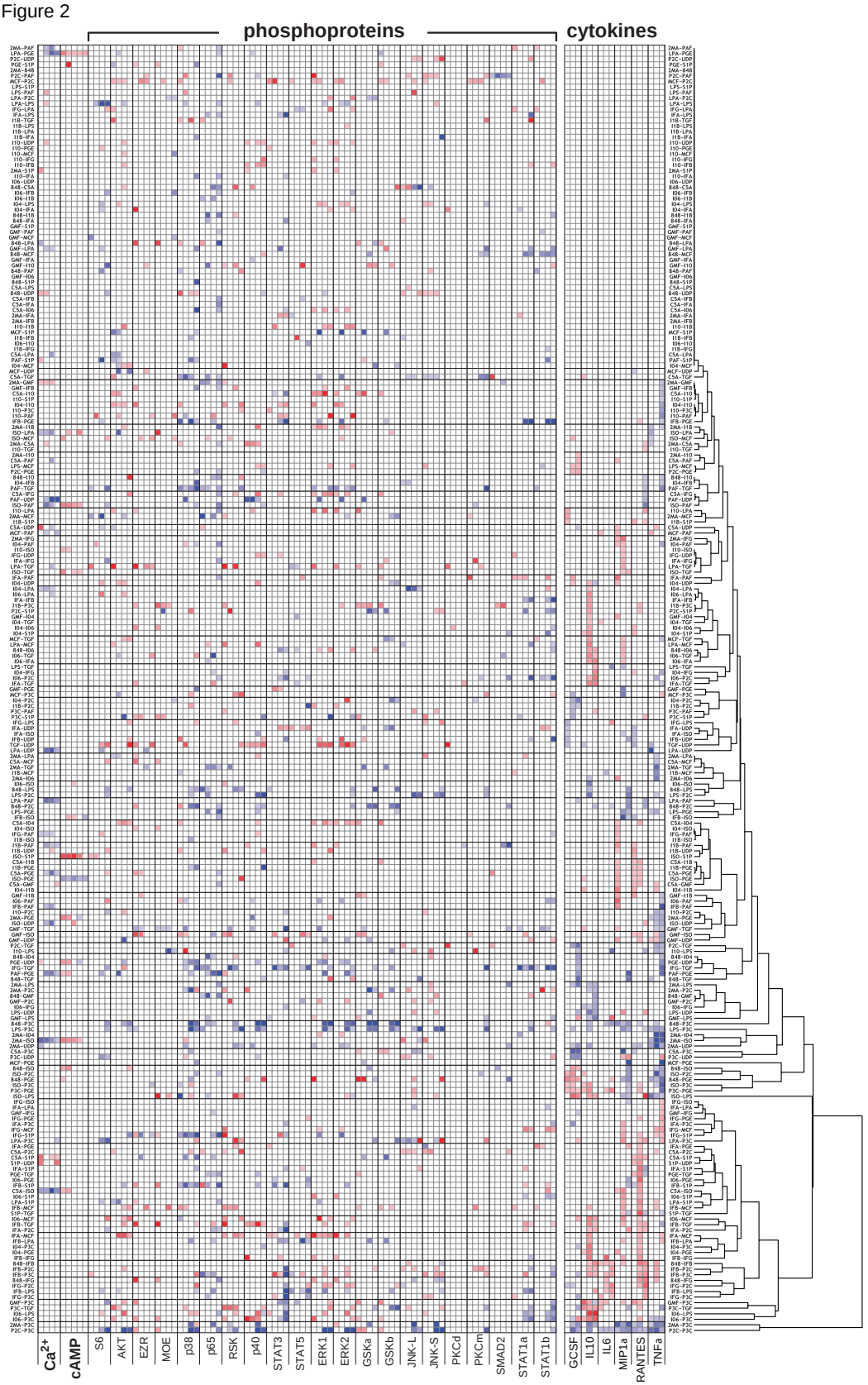

Figure S2 The double ligand screen for the RAW 264.7 macrophage. The two matrices shown represent the interactions between ligand pairs (rows) for all parameters (columns), that is, both early, rapid responses (larger matrix, left) and final cytokine outputs (right). For ease of comparison, the cytokine matrix on the right is the same matrix in Fig. 5, and calcium, cAMP, and protein phosphorylation responses are sorted by the ordering from the dendrogram in Fig. 5. Colorimetric representation is as in Fig. 5.

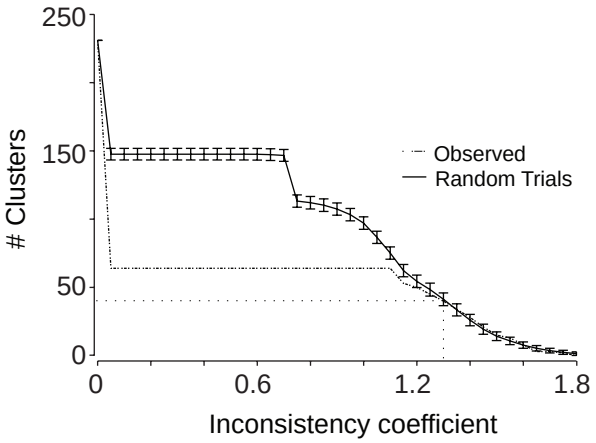

Figure S3 Identification of significant clusters. Inconsistency coefficients were calculated for each node in the dendrogram in Fig. 5. To identify the threshold of inconsistency coefficient above which clusters were deemed significant, we compared the number of clusters formed with different thresholds of inconsistency coefficients for the ΔΔZ matrix as well as for 1000 trials of randomly permuting the columns of the ΔΔZ matrix. The mean and standard deviation for the random matrices is shown as solid lines, while that for the experimentally observed data is shown as a dashed line. The deviation between the two traces signifies that the experimentally observed ΔΔZ matrix has fewer clusters than expected purely by chance. The inconsistency coefficient at the point of divergence (dotted lines) was used as the threshold for partitioning the ΔΔZ matrix into significant clusters.

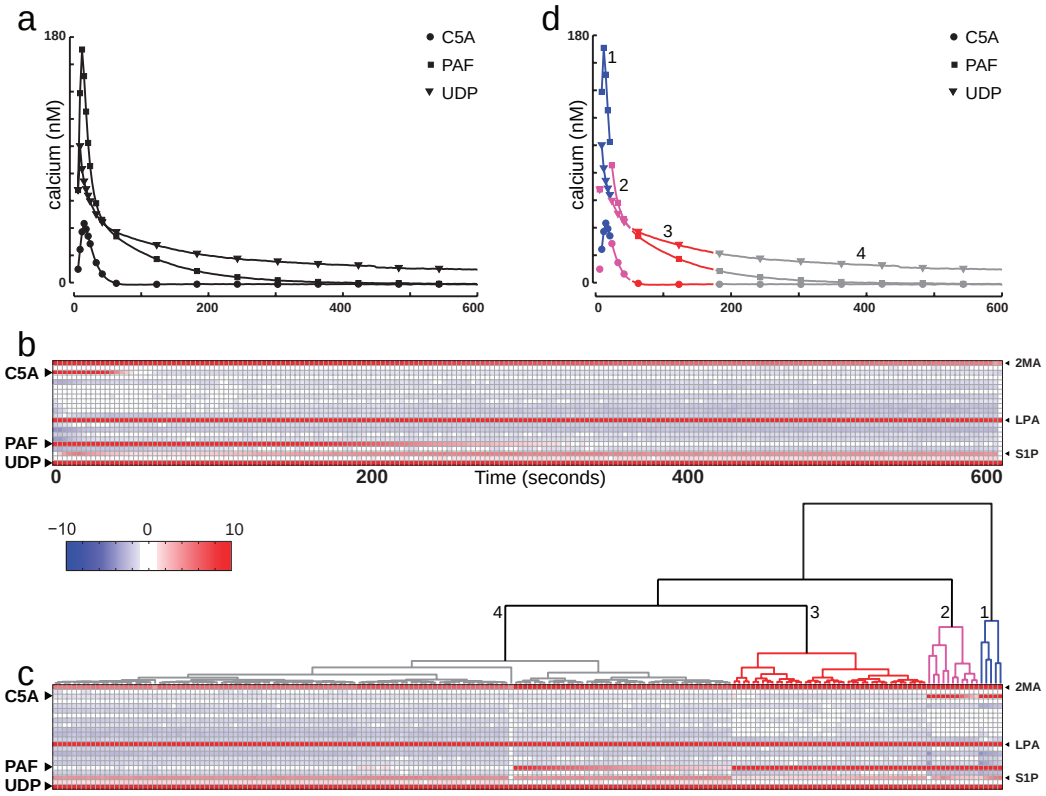

Figure S4 Data reduction (parameterization) of calcium. **a**, The calcium response to each ligand (representative ligands shown: C5A, PAF, UDP) was a timeseries measured every three seconds for 600 seconds (fewer symbols are shown for clarity). Ligands that produced a response had similar calcium profiles characterized by a large, rapid and transient increase followed in some cases (here, UDP alone) by a plateau phase of reduced magnitude. **b**, The matrix of Z-scores for calcium responses to all 22 ligands in the single ligand screen. The three ligands shown in **a** are labeled on the left of the matrix. Other ligands that had significant calcium responses are labeled on the right. Note how some responses (for example, LPA, UDP) are prolonged while others (for example, PAF, C5A) do not have the plateau phase. The color scale ranges from -10σ (blue) to +10σ (red) with insignificant values within ±1σ coloured white. **c**, The entire calcium matrix (all 22 ligands for 600 seconds) was hierarchically clustered by column (time-axis) to identify regions of the calcium time series that are naturally correlated across all the data and therefore might be reasonably averaged to provide a reduced parameter set. Four prominent clusters were identified (1-4, dendrogram colors blue, pink, red, gray respectively) by this method. **d**, Analysis of the clustered timeseries shows that the four clusters mostly correspond to contiguous sections of the calcium profile. Sections of the calcium trace corresponding to each of the four clusters are coded by color and labeled accordingly.

II. Supplementary Tables

Supplementary Table 1: The following 22 ligands were used in the AfCS ligand screens. These ligands were identified through search of the literature, identification of receptors by expression studies, and preliminary dose-response analysis. Detailed protocols for preparations of all ligands are listed on the AfCS website at http://www.signaling-gateway.org/data/cgi-bin/Protocols.cgi

Abbreviation	Ligand (with alternate names) and concentration
2MA	2-Methylthioadenosine 5'-triphosphate tetrasodium ; 2-methyl-thio-ATP; 500μM
848	Resiquimod (R-848); 100nM
C5A	Complement C5a, recombinant human; 100nM
GMF	Granulocyte-macrophage colony-stimulating factor, recombinant mouse, G-MCSF, 10pM.
IL-4	Interleukin-4, I04, IL4, recombinant mouse, 250pM
IL-6	Interleukin-6, I06, IL6, recombinant mouse, 300pM
IL-10	Interleukin 10, I10, IL10, recombinant human, 350pM
IL1β	Interleukin-1b, I1B, IL1b, recombinant mouse, 20pM
IFα	Interferon alpha, IFA, IFNa, recombinant mouse, 1nM
IFβ	Interferon beta, IFB, IFNb, recombinant mouse, 100pM
IFγ	Interferon gamma, IFG, IFNg, recombinant mouse, 300pM
ISO	Isoproterenol; isoprenaline, isopropylnoradrenaline , isopropterenol hydrochloride, 50nM
LPA	Lysophosphatidic acid, 1-oleoyl-2-hydroxy-sn-glycero-3-phosphate; 2.5μM
LPS	Lipopolysaccharide; 100ng/ml, with added LPS-binding protein (LBP) 250pM
MCF	Macrophage colony-stimulating factor, recombinant mouse; M-CSF; 200pM
P2C	Pam2Cys-SKKKK x 3 TFA; S-[2,3-bis(palmitoyloxy)-(2RS)-propyl]-[R]-cysteinyl-[S]-seryl-[S]-lysyl-[S]-lysyl-[S]-lysyl-[S]-lysine x 3 CF3COOH, PAM 2; 350nM
P3C	Pam3Cys-SKKKK x 3 HCl; (N-Palmitoyl-S-[2,3-bis(palmitoyloxy)-(2RS)-propyl]-[R]-cysteinyl-[S]-seryl-[S]-lysyl-[S]-lysyl-[S]-lysyl-[S]-lysine x 3 HCl), PAM 3; 1μM
PAF	Platelet activating factor, L-alpha-phosphatidylcholine, beta-acetyl-gamma-O-alkyl, 100nM
PGE	Prostaglandin E2, (5Z,11alpha,13E,15S)-11,15-Dihydroxy-9-oxoprosta-5,13-dienoic acid; 10μM
S1P	Sphingosine-1-phosphate; 1μM
TGFβ	Transforming growth factor-beta 1, recombinant human, Chinese hamster ovary cells; TGF-β1; TGF; TGFb; 10pM
UDP	Uridine 5'-diphosphate trisodium salt dihydrate; 25μM

Supplementary Table 2. Evidence for physiological relevance of co-stimulation of macrophage signaling pathways tested in this work in the context of immune signaling.

Ligands	Known mechanisms of endogenous production (immune context)	Co-stimulated pathways (immune context)
848 **LPS** **P2C** **P3C**	**Bacterial & PAMP Immune Signaling:** Stimulation of TLRs 1,2,4,6,7,8 mimics classic immune responses to bacteria, PAMPS, including specific microbial recognition[1-9].	Interacts with all other ligand groups tested. See below.
2MA **UDP**	**Purinergic agonists:** Adenosine analogs activating purinergic receptors. Endogenous ligands are ubiquitous – especially so in apoptotic environments[10-14].	**TLR:** Regulation of TLR-induced host cell damage; limit to inflammation[15, 16]. **Complement:** Chemotaxis; Recruitment of mast cells[17]. **Cytokines:** induces semi-maturation of dendritic cells by down-regulation of cytokines[18, 19].
C5A	**Complement Signaling:** Glycoproteins present in serum that are activated by immune complexes, bacterial activators etc. [20-22].	**TLR:** Adaptive Immune responses, phagocytosis and clearance in response to TLR stimulation[23, 24]. **Cytokines:** Known to augment opsonophagocytosis, clearance[25].
GMF **MCF**	**Cytokines – Colony Stimulating Factors:** activated by host defense responses to stimulate the proliferation of granulocyte and APC lineage cells [26, 27].	**TLR:** Innate immune responses [28-32]. **Cytokines:** With pro-inflammatory cytokines, promotes neutrophil extravasation and survival[33, 34]. **Cytokines – Interferons: R**egulates T-cell, macrophage differentiation by enhancing antigen presentation[35-37]. **Cytokines – TGFβ:** Synergy with TGFβ enhances granulopoiesis[38, 39].
IL4 **IL6** **IL10** **IL1β**	**Cytokines - Interleukins:** Produced by: IL1β-APCs; IL4-Th2 and mast cells; IL6-activated Th2 cells, APCs, other somatic cells[40]; IL10-activated Th2 cells, $CD8^+$ T and B cells, macrophages[41, 42]. Also seen in Fig. 1.	**TLR:** Negative regulation of TLR signaling; TLR-induced autocrine adaptors[31, 43-45]. **Cytokines- Interferons/TGFβ:** Regulation of production of other cytokines *in vitro*[39, 46-48]. **PAF:** IL1β enhances osteoclast survival through a PAF dependent pathway[49].
IFα **IFβ** **IFγ**	**Cytokines - Interferons:** Produced by: IFα/IFβ-APCs, neutrophils and some somatic cells; IFγ-activated Th1 and NK cells[50, 51]. Also seen in Fig. 1.	**TLR:** TLR-induced autocrine adaptors critical for effective innate responses, especially in viral signaling[52-55]. **PAF:** Endogenous synthesis/activation of PAF is necessary for mediating IFN-derived inflammatory responses[56].
TGFβ	**Cytokine:** Immune context: known anti-proliferative[57] produced by activated T(reg) cells, degranulating platelets at wound sites[58-60].	**TLR:** Regulation of TLR signaling – containment of inflammation[39, 61] **Phospholipids:** Overlaps and synergizes with S1P, LPA pathways[60, 62, 63].
LPA **S1P**	**Phospholipids:** Blood borne lysophospholipids that are primarily produced by activated platelets at wound sites[64-69].	**TLR:** Anti-inflammatory regulation[66, 67, 70]. **PAF:** Can induce PAF synthesis and enhance cellular migration[71].
PGE	Immune context: APCs produce AA-derived prostagladins including PGE upon TLR activation [64-66, 72-76].	**TLR:** Anti-inflammatory regulation[73, 77, 78]. **PAF:** Immune suppression[79].
PAF	**Lipid autocoid - GPCR (Gαq) activation:** Produced by endothelial cells, APCs, neutrophils, and plateles in response to endotoxin, hypoxia etc (thrombin activation)[80, 81].	**TLR:** Inflammation modulator[73, 81, 82].
ISO	**GPCR (Gαs) activation:** Classically found in all vasoactive areas. Recent studies show ubiquitous receptor expression in immune cells [83, 84].	**TLR:** Anti-inflammatory regulation[85].

Abbreviations used in the table: AA: Arachidonic acid; APC: Antigen-Presenting cells (macrophages and dendritic cells); NK: Natural Killer cells; Th1: T-cell helper Type 1; Th2: T-cell helper Type 2; PAMP: Pathogen Associated Molecular Patterns

III. Supplemental Methods:

Experiments described in this paper were performed in multiple AfCS laboratories. The AfCS Cell Preparation and Analysis Laboratory (Dallas, Director: P.C. Sternweis) produced uniform preparations of RAW 264.7 macrophages, executed all stimulation paradigms with them (i.e., incubations of cells with ligands) and obtained cellular extracts for further processing as necessary. Second messenger assays (Ca^{2+}, cAMP) were completed within the Cell Lab; appropriate cellular extracts are transferred to the Antibody Laboratory (Dallas, Director: S.M. Mumby) for subsequent assessment of phosphorylation of proteins and cytokine secretion. Data was deposited by each lab directly to central archives in the Bioinformatics Laboratory (UCSD, Director: S. Subramaniam) where they were parsed and made available to the public.

Culture of RAW 264.7 cells. (AfCS Procedure Protocol ID: PP00000159). RAW 264.7 cells are a macrophage-like cell line derived from BALB/c mice by transformation with Abelson leukaemia virus. RAW 264.7 cells were obtained from the American Type Culture Collection (ATCC; cat. no. TIB-71; lot no. 2263775), expanded, and stored in aliquots for use by AfCS laboratories (Preparation of Frozen Stocks of RAW 264.7 Cells, PP00000180). Stock vials of frozen AfCS cells are thawed using the Thaw Procedure for RAW 264.7 Cells (PP00000160).

Choice of Ligands. Supplementary Table 1 provides a list of the final 22 ligands used in the AfCS single and double ligand screens. Determination of ligands used in the screens was made through search of the literature, identification of receptors by expression studies, and preliminary dose-response analysis. Each ligand had to evoke significant responses in at least one measured output in the single ligand screen, and a dose response curve for the sentinel parameter was generated. Supplementary Figure 1 shows sample dose response curves for three ligands (UDP, ISO, IFβ) that induce among the

largest average calcium elevation, cAMP production and protein phosphorylation responses respectively. UDP increases intracellular calcium levels in a dose-dependent manner (Supplementary Fig. 1a). However, the peak of the calcium trace increased consistently with increasing ligand concentration (Supplementary Fig. 1b), and no saturation was observed. Accordingly, ligand doses from literature that were tested and confirmed within range in our experiments were selected; the concentration of UDP used in the single and double ligand screens was 25μM (indicated in bold and by arrowhead, Supplementary Fig. 1b).

Ligands stimulating cAMP yielded classic sigmoidal dose-response curves (e.g., ISO, Supplementary Fig. 1c). The ligand concentration selected (~80% max., 50nM for ISO as indicated in bold and by the arrowhead, Supplementary Fig. 1c) gives a robust response but is not close to saturation of the output assay – for instance, the cell is capable of producing vastly larger amounts of cAMP in the presence of ISO and S1P (see Fig. 2b).

All ligands that evoked changes in protein phosphorylation were tested at multiple times. For example, IFβ induced large changes in STAT3 phosphorylation (>100 fold over basal) 5 and 20 minutes after stimulation but at very different concentrations; simple selection of a concentration evoking a half-maximal response was not feasible. The final concentration used in the ligand screen was determined based on multiple parameters such as the maximum range of all responses, the least concentration of ligand needed to evoke a significant early response, and in consultation with the AfCS macrophage advisory committee. The phosphoprotein responses shown in Fig. 4d are among the largest observed in the single ligand screen. The ligand concentration used in the screen experiments (100pM for IFβ) is indicated in bold and by an arrowhead (Supplementary Fig. 1d).

Treatment Paradigms. Each experiment consisted of two individual treatments of single ligands and the simultaneous treatment of the ligand-pair. For only the calcium and cAMP assays, staggered additions of ligand were also performed. Treatment paradigms are described in greater detail below in the context of each individual assay.

Assay of Calcium. (AfCS Procedure Protocol ID: PP00000176). RAW cells that were grown overnight in 96-well plates were incubated with Fluo-3 (a Ca^{2+} sensitive fluorescent dye) and then washed to remove extra-cellular dye. Fluorescence was measured with a Fluoroskan Ascent (Thermo-Labsystems Fluoroskan). Resting levels of calcium (pre-treatment) were measured for at least 5 minutes; treatments with ligands were initiated by manual addition or automated dispensers. The following sequence was followed for individual ligands, combinations of ligands and vehicle controls (BUF): Treatment 1, response observation for 10 minutes; Treatment 2, response observation for an additional 10 minutes. For a given pair of ligands (L1 and L2), the treatment paradigms tested in parallel wells were (first addition : second addition respectively): [BUF : BUF], [L1 : L2], [L2 : L1], [L1&L2 simultaneously : BUF]. The single ligand survey was derived from single ligand controls (L1 alone or L2 alone, Treatment 1) from these experiments.

Assay of cAMP. (AfCS Procedure Protocol ID: PP00000175). An enzyme-linked immunoassay system (cAMP Biotrack EIA - Amersham Biosciences) was used to determine the intracellular levels of cAMP in untreated cells (0 min, baseline control) and in cells treated for 0.33, 0.67, 1.5, 5 and 20 minutes with ligands. Treatment paradigms were varied based on whether pairs of ligands were classified either as stimulators or non-stimulators of cAMP. For combinations where both ligands were stimulators, the treatment paradigms tested were for L1 alone, L2 alone, and L1 and L2 simultaneously. For combinations where one ligand did not stimulate cAMP, the non-stimulating ligand was not tested alone. Ligand pairs where neither ligand stimulated cAMP were not tested.

Assessment of phosphorylation of proteins. (AfCS Procedure Protocol ID: PP00000002-7, -142, -181, -258). Lysates of treated RAW 264.7 cells were separated through SDS-PAGE gels and immunoblotted with cocktails of phosphoprotein-specific antibody mixes. The phosphorylated states of the following proteins were recognized (site of phosphorylation in parenthesis): Akt (S473), ERK (T202/Y204), Ezrin/radixin/moesin (T567/T564/T558), GSK 3 α/β (S21/9), JNK (T183/Y185), p38 MAPK (T180/Y182), p40 phox (T154), ribosomal S6 (S235/236), NF-κB p65 (S536), PKC δ/θ (S643/676),

PKCμ (S916), p90 RSK (S380), Smad2 (S465/467), STAT 1 (Y701), STAT 3 (Y705), and STAT 5 (Y694). Measurements were made after 1, 3, 10, and 30 minutes of treatment with ligands; basal phosphorylation was assessed in untreated cells. Cells were treated with each individual ligand and simultaneously with the two ligand combination. There were no staggered additions of ligands. To correct for lane-to-lane variation in total protein loaded, all signal intensities are normalized against the signal for Rho-GDI detected by a phosphorylation insensitive antibody.

Measurement of Cytokines. (AfCS Procedure Protocol ID PP00000209, -221, -223). Secretion of cytokines into culture medium was measured using a Bio-Plex cytokine reagent kit (Bio-Plex mouse cytokine 18-plex panel: Bio-Rad). The cytokines recognized are: G-CSF, GM-CSF, IFN-γ, IL-1α, IL-1β, IL-2, IL-3, IL-4, IL-5, IL-6, IL-10, IL-12 (p40), IL-12 (p70), IL-17, KC, MIP-1α, RANTES, and TNFα. Measurements were made after 2, 3 and 4 hours of treatment with ligand; basal cytokine secretion was assessed in untreated cells at each of the above time points. Cells were treated with each individual ligand and simultaneously with the two ligand combination. Staggered or time-delayed stimulation with ligands were not performed.

Scaling and Normalization of Data: In any research study as large as the AfCS, systematic errors in measurement are inevitable despite rigorous control over experimental conditions in data acquisition. This can lead to considerable variability in data parameters; e.g., the variability in the peak calcium response among trials that use identical protocols for preparation and treatment of cells is significant, though the shape of the response is less variable. Similarly, the densitometric analysis of phosphoprotein western blots is subject to substantial variability for reasons ranging from differences in gel loading to variations in cell state. Some of this variability is reduced through systematic normalization against co-processed controls during experiments, but stochastic variability in ligand dose from mixing, non-linearities in instrument sensitivity, or buffering of signaling activities by indicator dyes require additional normalization steps. We normalized the cAMP, phosphoprotein, and cytokine datasets to the area under the curve of a mean response to stimulation, and guided by work from Flyvbjerg and Leibler[86], applied both peak amplitude and time-to-peak normalization to the

calcium datasets. These processing steps significantly improved the reproducibility of repeated trials of the same ligand while preserving the characteristic response shapes and the distinction between different ligands.

Reduction of Data.

1. Calcium: To adequately capture the information content of this assay without under-representing (eliminating valuable information) or over-representing (including redundant information) the data, we parameterized the calcium trace by an unbiased and unsupervised approach. We aligned the scaled, normalized mean calcium responses of all ligands, and clustered the data along the time dimension. This analysis seeks to identify the regions of the calcium time series that are naturally correlated across all the data and therefore might be reasonably consolidated to provide a reduced parameter set. Thus, four time segments were identified in the calcium datasets that could be used to identify unique profiles of response. Reassuringly, these cluster-derived time segments are fully consistent with expectation; they represent the initial rise to peak of calcium, the rapid decay of calcium transient, the slow decay to steady state, and the steady state (plateau) region (Supplementary Figure 4). Mechanistic studies support this decomposition of the calcium trace; sequential positive and negative feedback processes that act on the initial release of calcium are thought to control the rapid rise and rates of decay while molecularly distinct and slower influx processes control the plateau region [87, 88]. In short, we believe that the data-driven reduction of the calcium datasets provides an adequate representation of the underlying biology while minimizing the risk of over-representing this dataset in building the overall response profile for ligands.

2. Other Assays. While data reduction is useful in simplifying the data, it is also potentially dangerous in that it excludes data that may contain unanticipated information of value in discriminating ligand responses. It is therefore best applied conservatively - only when prior knowledge indicates it, or when the data clearly reveal a tight correlation of parameters. Thus, we did not attempt to reduce the datasets for cAMP, phosphoprotein, or release of cytokines, for which neither the literature nor the data itself support the averaging of measured parameters. Ultimately, the parameterization of the output profiles

for RAW 264.7 cells involved four parameters for calcium, five parameters for cAMP, 84 parameters for phosphoproteins, and 54 parameters for cytokines. Taken together, these constitute the 147 independent variables of the output profile for each ligand.

IV. Supplementary References:

1. Dunne, A. & O'Neill, L. A. Adaptor usage and Toll-like receptor signaling specificity. FEBS Lett 579, 3330-5 (2005).
2. O'Neill, L. A. How Toll-like receptors signal: what we know and what we don't know. Curr Opin Immunol 18, 3-9 (2006).
3. Akira, S., Yamamoto, M. & Takeda, K. Role of adapters in Toll-like receptor signalling. Biochem Soc Trans 31, 637-42 (2003).
4. Aravalli, R. N., Hu, S., Rowen, T. N., Palmquist, J. M. & Lokensgard, J. R. Cutting edge: TLR2-mediated proinflammatory cytokine and chemokine production by microglial cells in response to herpes simplex virus. J Immunol 175, 4189-93 (2005).
5. Kaisho, T. & Akira, S. Critical roles of Toll-like receptors in host defense. Crit Rev Immunol 20, 393-405 (2000).
6. Kaisho, T. & Akira, S. Toll-like receptors and their signaling mechanism in innate immunity. Acta Odontol Scand 59, 124-30 (2001).
7. Kaisho, T. & Akira, S. Toll-like receptors as adjuvant receptors. Biochim Biophys Acta 1589, 1-13 (2002).
8. Cristofaro, P. & Opal, S. M. Role of Toll-like receptors in infection and immunity: clinical implications. Drugs 66, 15-29 (2006).
9. Horng, T., Barton, G. M., Flavell, R. A. & Medzhitov, R. The adaptor molecule TIRAP provides signalling specificity for Toll-like receptors. Nature 420, 329-33 (2002).
10. Cronstein, B. N. Adenosine, an endogenous anti-inflammatory agent. J Appl Physiol 76, 5-13 (1994).
11. Burnstock, G. Pathophysiology and therapeutic potential of purinergic signaling. Pharmacol Rev 58, 58-86 (2006).
12. Chen, L. & Brosnan, C. F. Exacerbation of experimental autoimmune encephalomyelitis in P2X7R-/- mice: Evidence for loss of apoptotic activity in lymphocytes. J Immunol 176, 3115-26 (2006).
13. Lepine, S., Le Stunff, H., Lakatos, B., Sulpice, J. C. & Giraud, F. ATP-induced apoptosis of thymocytes is mediated by activation of P2X7 receptor and involves de novo ceramide synthesis and mitochondria. Biochim Biophys Acta 1761, 73-82 (2006).
14. Stefanelli, C. et al. ATP depletion inhibits glucocorticoid-induced thymocyte apoptosis. Biochem J 322 (Pt 3), 909-17 (1997).
15. Kaufmann, A. et al. "Host tissue damage" signal ATP promotes non-directional migration and negatively regulates toll-like receptor signaling in human monocytes. J Biol Chem 280, 32459-67 (2005).
16. Feng, C., Mery, A. G., Beller, E. M., Favot, C. & Boyce, J. A. Adenine nucleotides inhibit cytokine generation by human mast cells through a Gs-coupled receptor. J Immunol 173, 7539-47 (2004).
17. McCloskey, M. A., Fan, Y. & Luther, S. Chemotaxis of rat mast cells toward adenine nucleotides. J Immunol 163, 970-7 (1999).
18. Marteau, F., Communi, D., Boeynaems, J. M. & Suarez Gonzalez, N. Involvement of multiple P2Y receptors and signaling pathways in the action of adenine nucleotides diphosphates on human monocyte-derived dendritic cells. J Leukoc Biol 76, 796-803 (2004).
19. Horckmans, M. et al. Extracellular adenine nucleotides inhibit the release of major monocyte recruiters by human monocyte-derived dendritic cells. FEBS Lett 580, 747-54 (2006).
20. Thurman, J. M. & Holers, V. M. The central role of the alternative complement pathway in human disease. J Immunol 176, 1305-10 (2006).
21. Kim, S. J., Gershov, D., Ma, X., Brot, N. & Elkon, K. B. Opsonization of apoptotic cells and its effect on macrophage and T cell immune responses. Ann N Y Acad Sci 987, 68-78 (2003).

22. Roos, A. et al. Mini-review: A pivotal role for innate immunity in the clearance of apoptotic cells. Eur J Immunol 34, 921-9 (2004).
23. Hawlisch, H. & Kohl, J. Complement and Toll-like receptors: key regulators of adaptive immune responses. Mol Immunol 43, 13-21 (2006).
24. Kirimanjeswara, G. S., Mann, P. B., Pilione, M., Kennett, M. J. & Harvill, E. T. The complex mechanism of antibody-mediated clearance of Bordetella from the lungs requires TLR4. J Immunol 175, 7504-11 (2005).
25. Campbell, J. R. & Edwards, M. S. Cytokines enhance opsonophagocytosis of type III group B Streptococcus. J Perinatol 20, 225-30 (2000).
26. Chitu, V. & Stanley, E. R. Colony-stimulating factor-1 in immunity and inflammation. Curr Opin Immunol 18, 39-48 (2006).
27. Hamilton, J. A. & Anderson, G. P. GM-CSF Biology. Growth Factors 22, 225-31 (2004).
28. Bozinovski, S. et al. Innate immune responses to LPS in mouse lung are suppressed and reversed by neutralization of GM-CSF via repression of TLR-4. Am J Physiol Lung Cell Mol Physiol 286, L877-85 (2004).
29. Kurt-Jones, E. A. et al. Role of toll-like receptor 2 (TLR2) in neutrophil activation: GM-CSF enhances TLR2 expression and TLR2-mediated interleukin 8 responses in neutrophils. Blood 100, 1860-8 (2002).
30. Takami, M., Kim, N., Rho, J. & Choi, Y. Stimulation by toll-like receptors inhibits osteoclast differentiation. J Immunol 169, 1516-23 (2002).
31. Chano, F. & Descoteaux, A. Modulation of lipopolysaccharide-induced NF-IL6 activation by protein kinase C-alpha in a mouse macrophage cell line. Eur J Immunol 32, 2897-904 (2002).
32. Krutzik, S. R. et al. TLR activation triggers the rapid differentiation of monocytes into macrophages and dendritic cells. Nat Med 11, 653-60 (2005).
33. Smith, W. B., Gamble, J. R. & Vadas, M. A. The role of granulocyte-macrophage and granulocyte colony-stimulating factors in neutrophil transendothelial migration: comparison with interleukin-8. Exp Hematol 22, 329-34 (1994).
34. McGettrick, H. M. et al. Chemokine- and adhesion-dependent survival of neutrophils after transmigration through cytokine-stimulated endothelium. J Leukoc Biol (2006).
35. Rohrschneider, L. R. et al. Growth and differentiation signals regulated by the M-CSF receptor. Mol Reprod Dev 46, 96-103 (1997).
36. Dauffy, J., Mouchiroud, G. & Bourette, R. P. The interferon-inducible gene, Ifi204, is transcriptionally activated in response to M-CSF, and its expression favors macrophage differentiation in myeloid progenitor cells. J Leukoc Biol 79, 173-83 (2006).
37. Ahlers, J. D., Belyakov, I. M., Matsui, S. & Berzofsky, J. A. Mechanisms of cytokine synergy essential for vaccine protection against viral challenge. Int Immunol 13, 897-908 (2001).
38. Keller, J. R., Jacobsen, S. E., Sill, K. T., Ellingsworth, L. R. & Ruscetti, F. W. Stimulation of granulopoiesis by transforming growth factor beta: synergy with granulocyte/macrophage-colony-stimulating factor. Proc Natl Acad Sci U S A 88, 7190-4 (1991).
39. Li, M. O., Wan, Y. Y., Sanjabi, S., Robertson, A. K. & Flavell, R. A. TRANSFORMING GROWTH FACTOR-beta REGULATION OF IMMUNE RESPONSES. Annu Rev Immunol 24, 99-146 (2006).
40. Kishimoto, T. Interleukin-6: from basic science to medicine--40 years in immunology. Annu Rev Immunol 23, 1-21 (2005).
41. Moore, K. W., de Waal Malefyt, R., Coffman, R. L. & O'Garra, A. Interleukin-10 and the interleukin-10 receptor. Annu Rev Immunol 19, 683-765 (2001).
42. Pestka, S. et al. Interleukin-10 and related cytokines and receptors. Annu Rev Immunol 22, 929-79 (2004).
43. Liew, F. Y., Xu, D., Brint, E. K. & O'Neill, L. A. Negative regulation of toll-like receptor-mediated immune responses. Nat Rev Immunol 5, 446-58 (2005).

44. Netea, M. G. et al. Toll-like receptor 2 suppresses immunity against Candida albicans through induction of IL-10 and regulatory T cells. J Immunol 172, 3712-8 (2004).
45. Schilling, D., Thomas, K., Nixdorff, K., Vogel, S. N. & Fenton, M. J. Toll-like receptor 4 and Toll-IL-1 receptor domain-containing adapter protein (TIRAP)/myeloid differentiation protein 88 adapter-like (Mal) contribute to maximal IL-6 expression in macrophages. J Immunol 169, 5874-80 (2002).
46. Howells, G., Pham, P., Taylor, D., Foxwell, B. & Feldmann, M. Interleukin 4 induces interleukin 6 production by endothelial cells: synergy with interferon-gamma. Eur J Immunol 21, 97-101 (1991).
47. Hedges, S. R., Bjarnadottir, M., Agace, W., Hang, L. & Svanborg, C. Immunoregulatory cytokines modify Escherichia coli induced uroepithelial cell IL-6 and IL-8 responses. Cytokine 8, 686-97 (1996).
48. McGee, D. W., Beagley, K. W., Aicher, W. K. & McGhee, J. R. Transforming growth factor-beta and IL-1 beta act in synergy to enhance IL-6 secretion by the intestinal epithelial cell line, IEC-6. J Immunol 151, 970-8 (1993).
49. Hikiji, H., Ishii, S., Shindou, H., Takato, T. & Shimizu, T. Absence of platelet-activating factor receptor protects mice from osteoporosis following ovariectomy. J Clin Invest 114, 85-93 (2004).
50. Sen, G. C. Viruses and interferons. Annu Rev Microbiol 55, 255-81 (2001).
51. Pestka, S., Krause, C. D. & Walter, M. R. Interferons, interferon-like cytokines, and their receptors. Immunol Rev 202, 8-32 (2004).
52. Bowie, A. G. & Haga, I. R. The role of Toll-like receptors in the host response to viruses. Mol Immunol 42, 859-67 (2005).
53. Hertzog, P. J., O'Neill, L. A. & Hamilton, J. A. The interferon in TLR signaling: more than just antiviral. Trends Immunol 24, 534-9 (2003).
54. Gao, J. J. et al. Autocrine/paracrine IFN-alphabeta mediates the lipopolysaccharide-induced activation of transcription factor Stat1alpha in mouse macrophages: pivotal role of Stat1alpha in induction of the inducible nitric oxide synthase gene. J Immunol 161, 4803-10 (1998).
55. Riches, D. W. & Underwood, G. A. Expression of interferon-beta during the triggering phase of macrophage cytocidal activation. Evidence for an autocrine/paracrine role in the regulation of this state. J Biol Chem 266, 24785-92 (1991).
56. Talvani, A. et al. Experimental Trypanosoma cruzi infection in platelet-activating factor receptor-deficient mice. Microbes Infect 5, 789-96 (2003).
57. Peng, Y., Gorelik, L., Laouar, Y., Li, M. O. & Flavell, R. A. TGFbeta-mediated immunoregulation. Ernst Schering Res Found Workshop, 155-60 (2006).
58. Akdis, M., Blaser, K. & Akdis, C. A. T regulatory cells in allergy. Chem Immunol Allergy 91, 159-73 (2006).
59. Taylor, A., Verhagen, J., Blaser, K., Akdis, M. & Akdis, C. A. Mechanisms of immune suppression by interleukin-10 and transforming growth factor-beta: the role of T regulatory cells. Immunology 117, 433-42 (2006).
60. Sauer, B. et al. Involvement of Smad signaling in sphingosine 1-phosphate-mediated biological responses of keratinocytes. J Biol Chem 279, 38471-9 (2004).
61. Lucas, M., Stuart, L. M., Savill, J. & Lacy-Hulbert, A. Apoptotic cells and innate immune stimuli combine to regulate macrophage cytokine secretion. J Immunol 171, 2610-5 (2003).
62. Radeke, H. H. et al. Overlapping signaling pathways of sphingosine 1-phosphate and TGF-beta in the murine Langerhans cell line XS52. J Immunol 174, 2778-86 (2005).
63. Sauer, B. et al. Lysophosphatidic acid interacts with transforming growth factor-beta signaling to mediate keratinocyte growth arrest and chemotaxis. J Invest Dermatol 123, 840-9 (2004).
64. Dieter, P., Kolada, A., Kamionka, S., Schadow, A. & Kaszkin, M. Lipopolysaccharide-induced release of arachidonic acid and prostaglandins in liver macrophages: regulation by Group IV

cytosolic phospholipase A2, but not by Group V and Group IIA secretory phospholipase A2. Cell Signal 14, 199-204 (2002).
65. Kim, Y. S. et al. Glutamine inhibits lipopolysaccharide-induced cytoplasmic phospholipase A2 activation and protects against endotoxin shock in mouse. Shock 25, 290-4 (2006).
66. Peng, X. et al. Protective effects of sphingosine 1-phosphate in murine endotoxin-induced inflammatory lung injury. Am J Respir Crit Care Med 169, 1245-51 (2004).
67. Ishii, I., Fukushima, N., Ye, X. & Chun, J. Lysophospholipid receptors: signaling and biology. Annu Rev Biochem 73, 321-54 (2004).
68. Sanna, M. G. et al. Sphingosine 1-phosphate (S1P) receptor subtypes S1P1 and S1P3, respectively, regulate lymphocyte recirculation and heart rate. J Biol Chem 279, 13839-48 (2004).
69. Yatomi, Y., Ozaki, Y., Ohmori, T. & Igarashi, Y. Sphingosine 1-phosphate: synthesis and release. Prostaglandins Other Lipid Mediat 64, 107-22 (2001).
70. McVerry, B. J. & Garcia, J. G. In vitro and in vivo modulation of vascular barrier integrity by sphingosine 1-phosphate: mechanistic insights. Cell Signal 17, 131-9 (2005).
71. Bernatchez, P. N., Tremblay, F., Rollin, S., Neagoe, P. E. & Sirois, M. G. Sphingosine 1-phosphate effect on endothelial cell PAF synthesis: role in cellular migration. J Cell Biochem 90, 719-31 (2003).
72. Guastadisegni, C., Nicolini, A., Balduzzi, M., Ajmone-Cat, M. A. & Minghetti, L. Modulation of PGE(2) and TNFalpha by nitric oxide and LPS-activated RAW 264.7 cells. Cytokine 19, 175-80 (2002).
73. Jiang, Y. J., Lu, B., Choy, P. C. & Hatch, G. M. Regulation of cytosolic phospholipase A2, cyclooxygenase-1 and -2 expression by PMA, TNFalpha, LPS and M-CSF in human monocytes and macrophages. Mol Cell Biochem 246, 31-8 (2003).
74. Jin, S. L., Lan, L., Zoudilova, M. & Conti, M. Specific role of phosphodiesterase 4B in lipopolysaccharide-induced signaling in mouse macrophages. J Immunol 175, 1523-31 (2005).
75. Sautebin, L. et al. Cyclooxygenase-2-dependent generation of 8-epiprostaglandin F2alpha by lipopolysaccharide-activated J774 macrophages. Inflamm Res 48, 503-8 (1999).
76. Vivancos, M. & Moreno, J. J. Role of Ca(2+)-independent phospholipase A(2) and cyclooxygenase/lipoxygenase pathways in the nitric oxide production by murine macrophages stimulated by lipopolysaccharides. Nitric Oxide 6, 255-62 (2002).
77. Hareng, L., Meergans, T., von Aulock, S., Volk, H. D. & Hartung, T. Cyclic AMP increases endogenous granulocyte colony-stimulating factor formation in monocytes and THP-1 macrophages despite attenuated TNF-alpha formation. Eur J Immunol 33, 2287-96 (2003).
78. Lukashev, D., Ohta, A., Apasov, S., Chen, J. F. & Sitkovsky, M. Cutting edge: Physiologic attenuation of proinflammatory transcription by the Gs protein-coupled A2A adenosine receptor in vivo. J Immunol 173, 21-4 (2004).
79. Walterscheid, J. P., Ullrich, S. E. & Nghiem, D. X. Platelet-activating factor, a molecular sensor for cellular damage, activates systemic immune suppression. J Exp Med 195, 171-9 (2002).
80. Meyer, M. C., Rastogi, P., Beckett, C. S. & McHowat, J. Phospholipase A2 inhibitors as potential anti-inflammatory agents. Curr Pharm Des 11, 1301-12 (2005).
81. Zimmerman, G. A., McIntyre, T. M., Prescott, S. M. & Stafforini, D. M. The platelet-activating factor signaling system and its regulators in syndromes of inflammation and thrombosis. Crit Care Med 30, S294-301 (2002).
82. Ferreira, M. A. et al. Sponge-induced angiogenesis and inflammation in PAF receptor-deficient mice (PAFR-KO). Br J Pharmacol 141, 1185-92 (2004).
83. Bergmann, M. & Sautner, T. Immunomodulatory effects of vasoactive catecholamines. Wien Klin Wochenschr 114, 752-61 (2002).

84. Kohm, A. P. & Sanders, V. M. Norepinephrine and beta 2-adrenergic receptor stimulation regulate CD4+ T and B lymphocyte function in vitro and in vivo. Pharmacol Rev 53, 487-525 (2001).
85. Zhang, H. et al. Effect of adrenoreceptors on endotoxin-induced cytokines and lipid peroxidation in lung explants. Am J Respir Crit Care Med 160, 1703-10 (1999).
86. Flyvbjerg, H., Jobs, E. & Leibler, S. Kinetics of self-assembling microtubules: an "inverse problem" in biochemistry. Proc Natl Acad Sci U S A 93, 5975-9 (1996).
87. Goldbeter, A., Dupont, G. & Berridge, M. J. Minimal model for signal-induced Ca2+ oscillations and for their frequency encoding through protein phosphorylation. Proc Natl Acad Sci U S A 87, 1461-5 (1990).
88. Dupont, G., Berridge, M. J. & Goldbeter, A. Latency correlates with period in a model for signal-induced Ca2+ oscillations based on Ca2(+)-induced Ca2+ release. Cell Regul 1, 853-61 (1990).